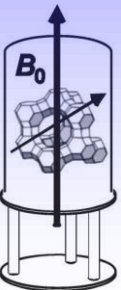


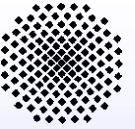
# *Mechanisms and State of the Art of Methanol-to-hydrocarbon (MTH) Conversion on Acidic Zeolite Catalysts*

Michael Hunger

Institute of Chemical Technology  
University of Stuttgart, Germany

Evonik, Hanau, January 13, 2012





## ***History of methanol-to-hydrocarbon (MTH) conversion on zeolites***

### **MTG (methanol-to-gasoline):**

- 1982, Wesseling/Germany, demonstration plant, 6 870 t gasoline, H-ZSM-5, total process time 8 600 h, later modified to MTO process
- 1986, Maui field/New Zealand, commercial process, 600 000 t gasoline per year, H-ZSM-5, stopped after ca. 5 years

### **MTO (methanol-to-olefin):**

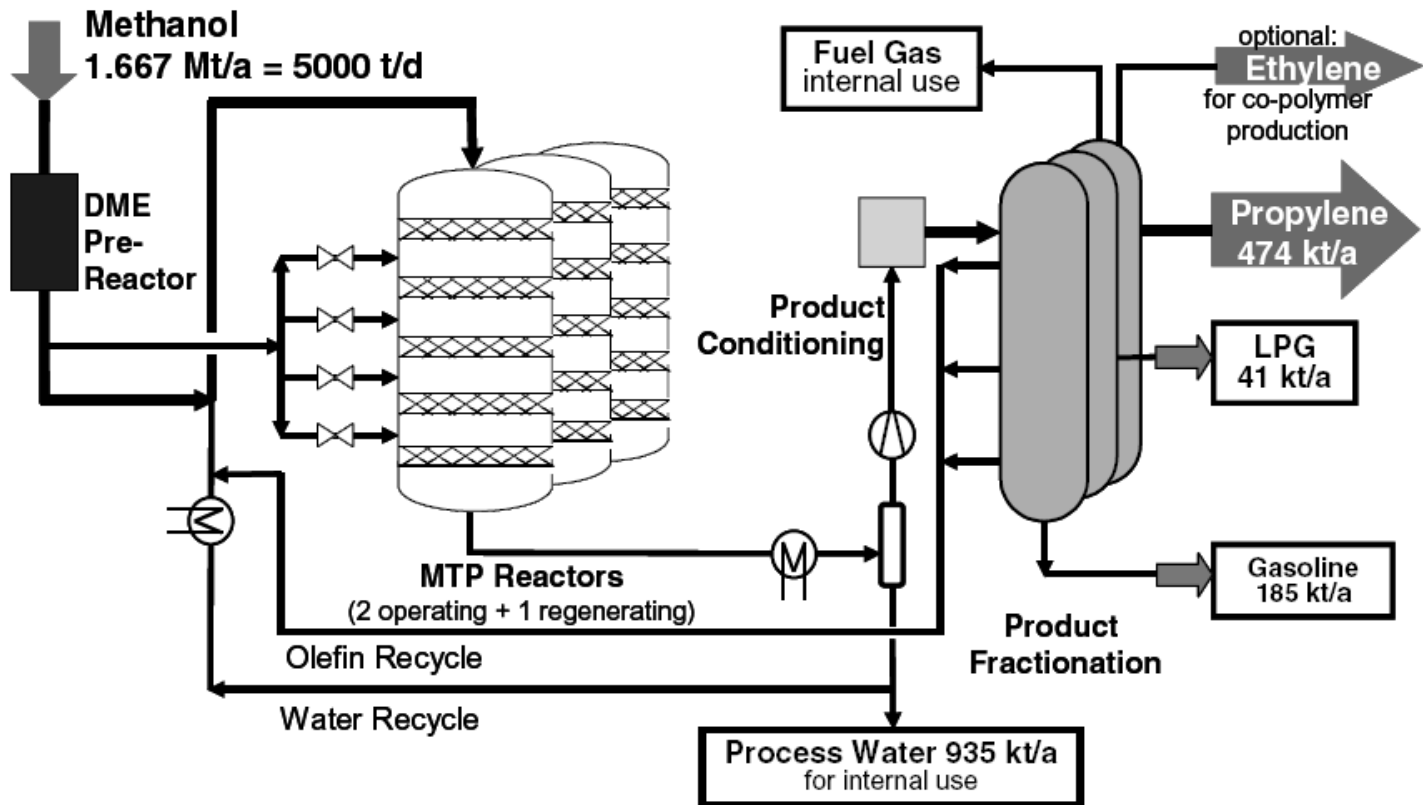
- 1996, Norsk Hydro/Norway, demonstration unit, 0.5 t ethene and propene per year, H-SAPO-34
- 2005, Dalian/VR China, test unit, 10 000 t olefins per year, and Shaanxi/VR China, start of the construction of a commercial plant, 800 000 t olefins per year

### **MTP (methanol-to-propylene):**

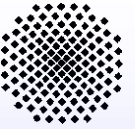
- 2005 to 2011, Lurgi signed three contracts for MTP plants in VR China
- 2012, Ningdong/VR China, Lurgi's MTP-1 plant (500.000 t methanol per year) will be completed



## Lurgi's MTP process



- ZSM-5 catalyst of Süd-Chemie AG with lifetime of 500-600 h
- two parallel MTP reactors, one for regeneration
- propylene purity of 97 % is reached after cold box system and recycling of process water and C<sub>2</sub> plus C<sub>4+</sub> olefins

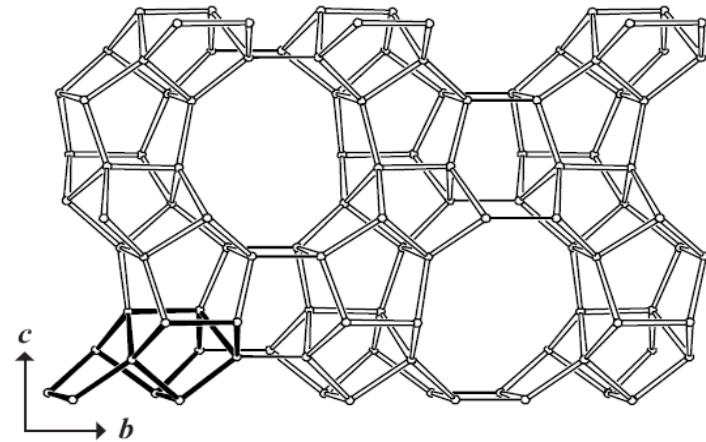


## **Zeolite catalysts applied for the methanol conversion**

### **H-ZSM-5: Structure type MFI**

$\text{H}^+ \text{n}[\text{Al}_n \text{Si}_{96-n} \text{O}_{192}]$

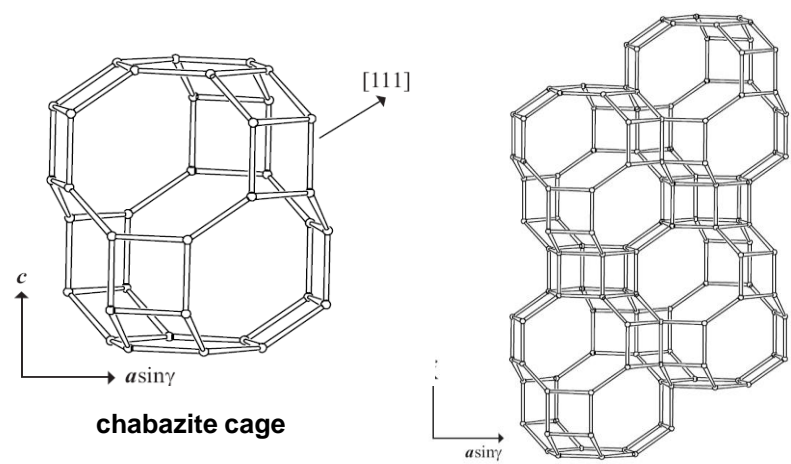
crossing intersections at  
interconnecting 10-ring channels  
[100] 0.51 nm x 0.55 nm  
[010] 0.53 nm x 0.56 nm

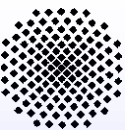


### **H-SAPO-34: Structure type CHA**

$\text{H}^+ \text{n}[\text{Al}_{18} \text{P}_{18-n} \text{Si}_n \text{O}_{72}]$

chabazite cages accessible by  
8-ring windows perpendicular to  
[001] 0.38 nm x 0.38 nm





## ***Periods in the life of an MTH catalysts***

### ***I: Induction period of the methanol conversion on zeolites***

formation of first C-C bonds by decomposition of surface methoxy groups or alkylation of organic impurities



### ***II: Steady-state of the methanol conversion on zeolites***

methylation and dealkylation of organic compounds forming a catalytically active hydrocarbon pool



### ***III: Catalyst deactivation during methanol conversion on zeolites***

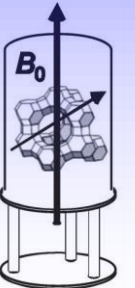
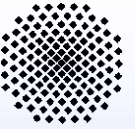
formation of inactive coke deposits affecting the methanol conversion and the selectivity to ethylene and propylene



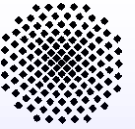
### ***IV: Catalyst regeneration***

burning of coke deposits, which block the pores and acid sites, by high-temperature treatment mostly in air





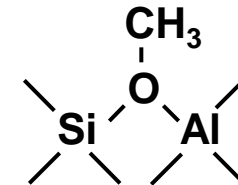
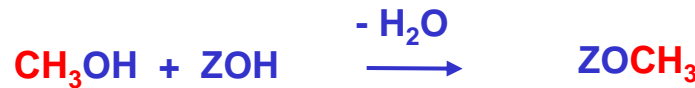
## *I. The induction period of the MTO reaction on acidic zeolite catalysts*



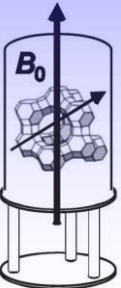
## I: Induction period

formation of catalytically active organic deposits in zeolite pores (hydrocarbon-pool compounds):

- impurities in the methanol feed may act as organic precursors
- formation of surface methoxy groups



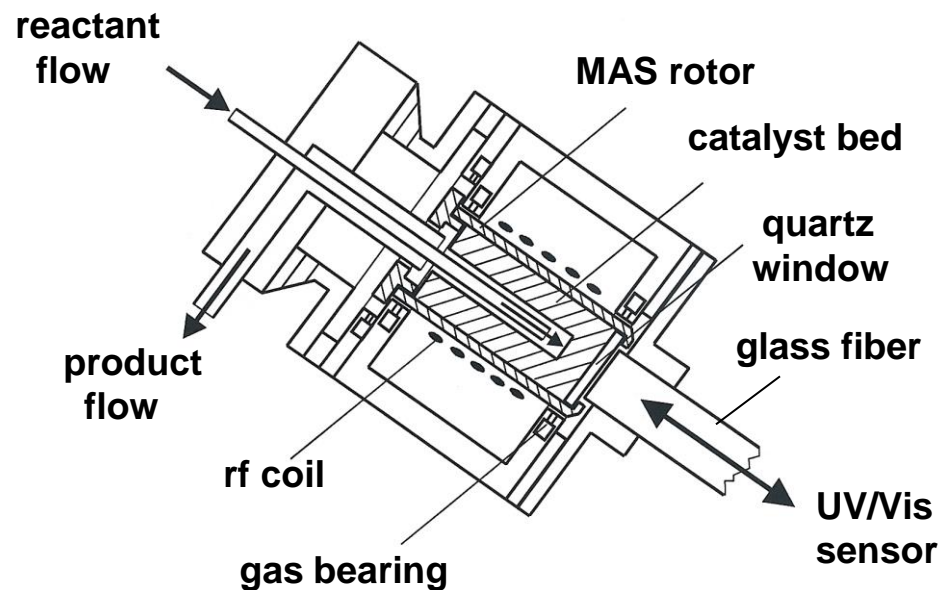
- decomposition of surface methoxy groups leads to first C-C bond formation and methylation of hydrocarbons
- alkylation of organic precursors leads to the formation of hydrocarbon-pool compounds (alkylated olefins and aromatics)



## I: Induction period

MAS NMR-UV/Vis studies of the decomposition of methoxy groups on H-Y and H-SAPO-34 formed by methanol

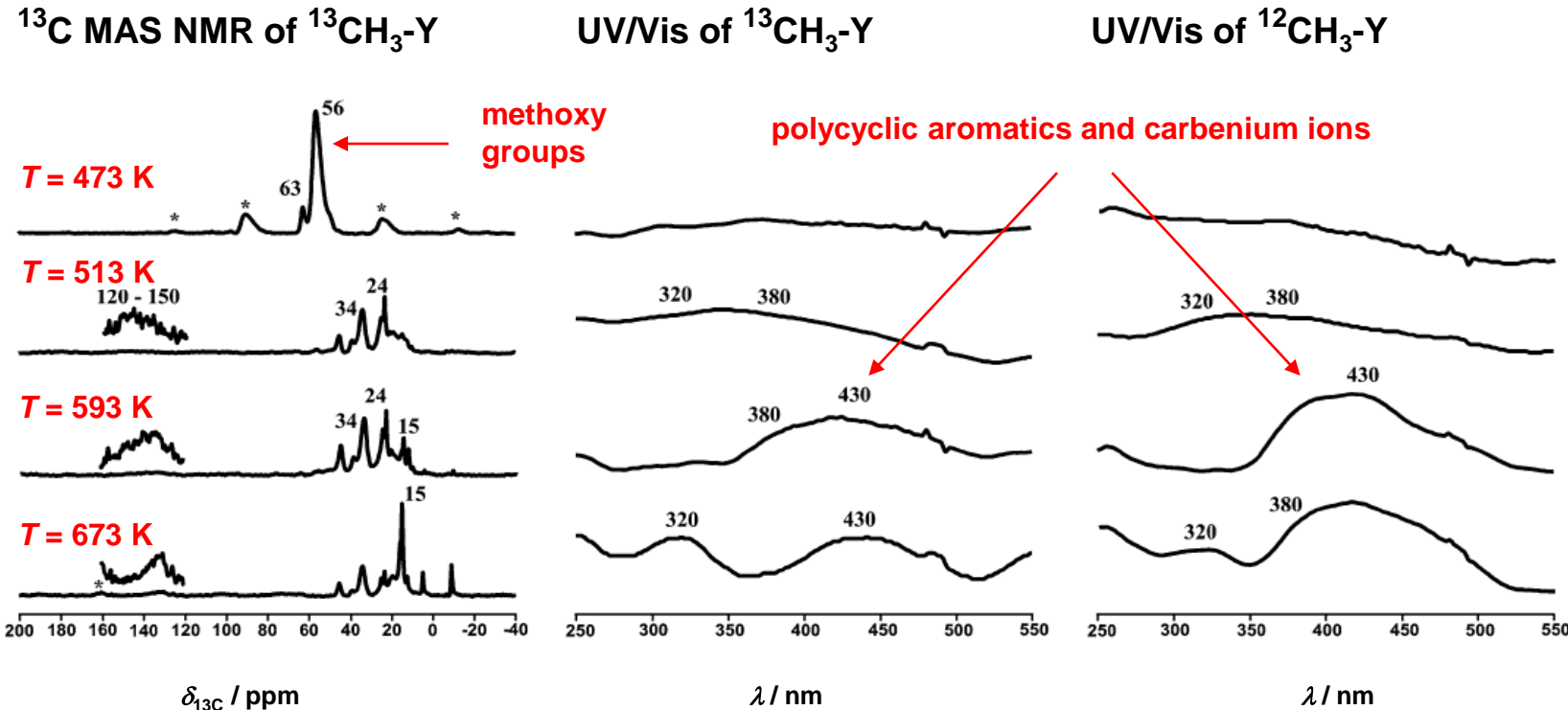
- experimental technique:  
M. Hunger, W. Wang,  
Chem. Commun. (2004)  
584



- preparation of methoxy groups by adsorption of  $^{13}\text{C}$ -enriched methanol and highly purified (impurities < 30 ppm)  $^{12}\text{CH}_3\text{OH}$  on H-Y and H-SAPO-34 and thermal treatment

# I: Induction period

*in situ* MAS NMR-UV/Vis study of the decomposition of methoxy groups

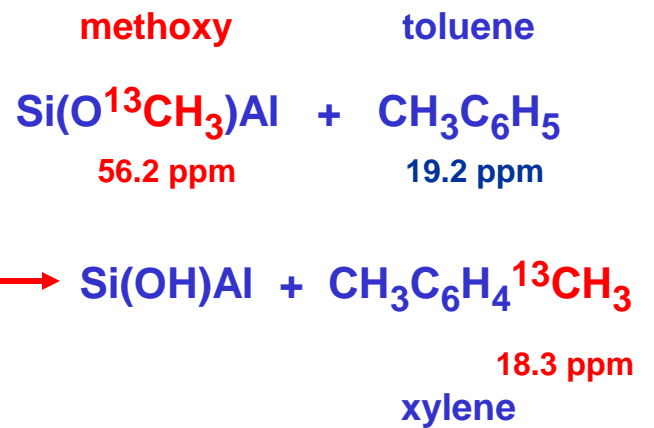
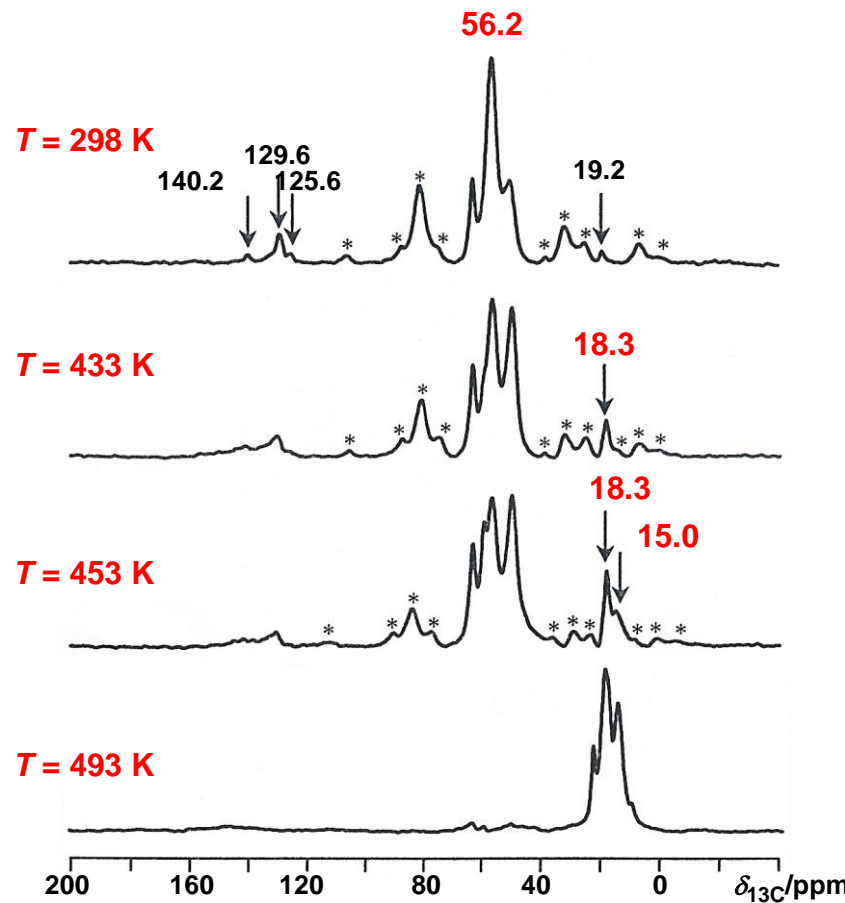


- decomposition of methoxy groups formed by  $^{13}\text{C}$ -enriched and highly purified (impurities < 30 ppm) methanol start at the same temperature and give similar UV/Vis-sensitive hydrocarbons
- first hydrocarbons can be formed via alkoxy route

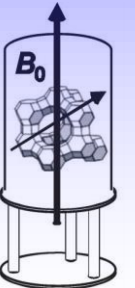
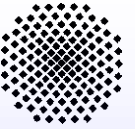
## I: Induction period

reaction of methoxy groups with toluene on zeolite H-Y

$^{13}\text{C}$  stopped-flow MAS NMR



- methoxy groups contribute to the alkylation of aromatic compounds

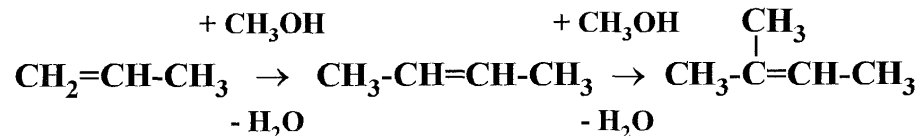


## *II. Steady-state of the methanol conversion on acidic zeolites*

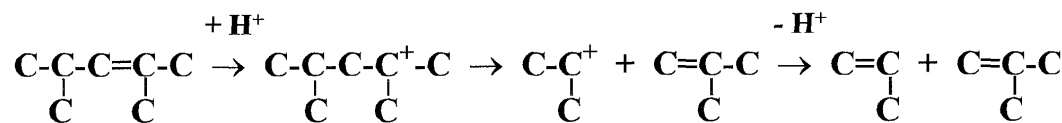
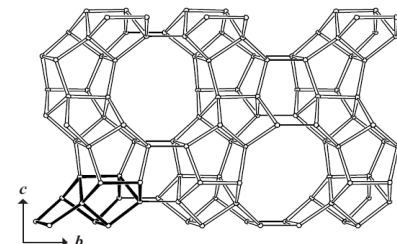
## II: Steady-state conditions

most favored reaction mechanism is the hydrocarbon-pool mechanism:

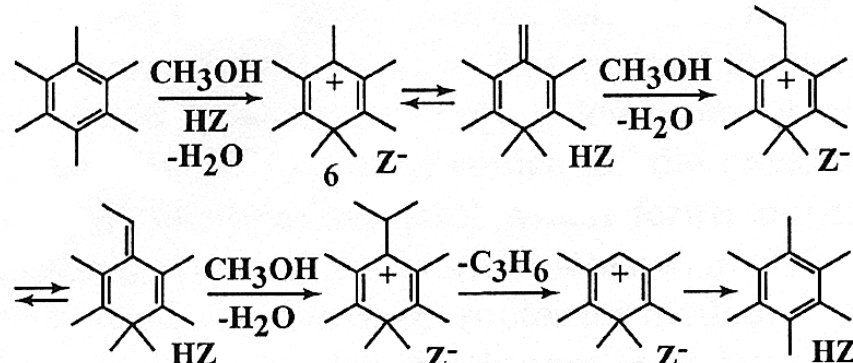
- via olefinic compounds (H. Schulz, M. Wei, Microporous Mesoporous Mater. 29 (1999) 205)



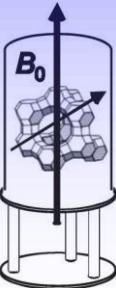
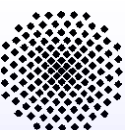
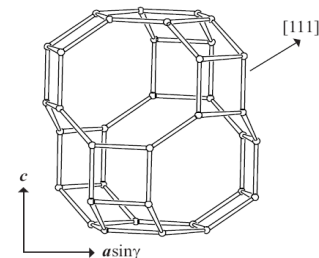
H-ZSM-5



- via polyalkylaromatics (J.F. Haw et al., Acc. Chem. Res. 36 (2003) 317)

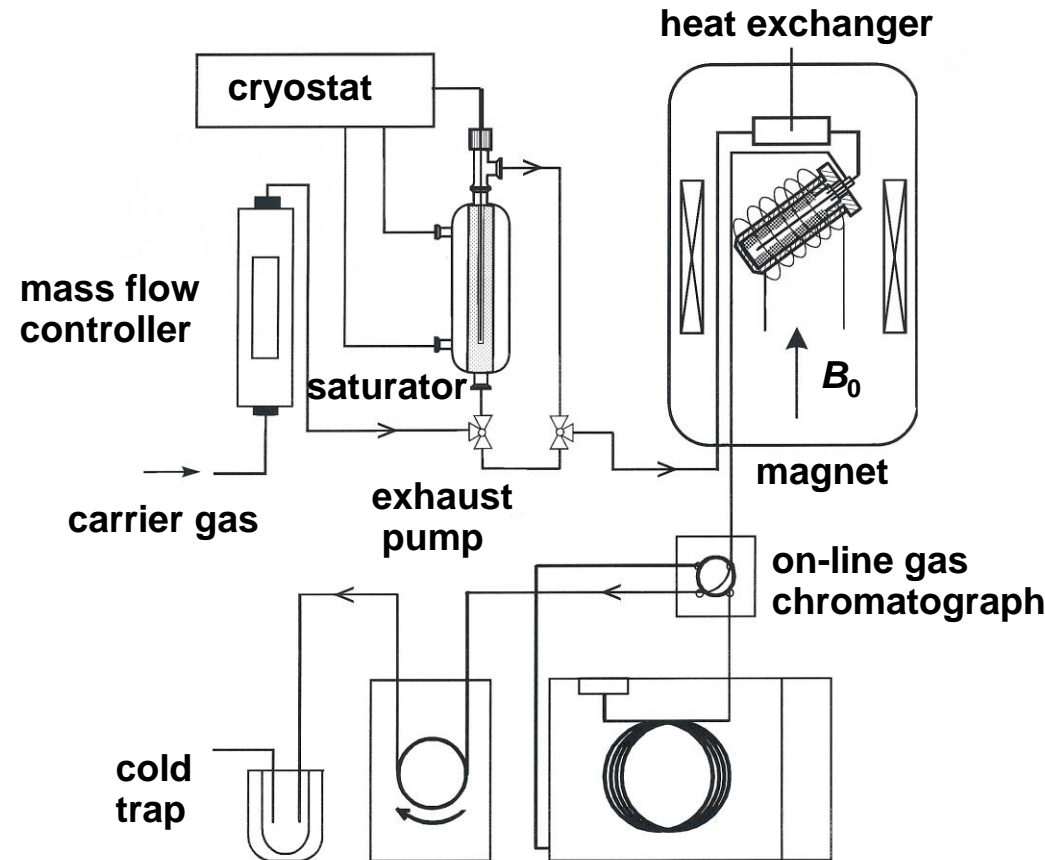


SAPO-34



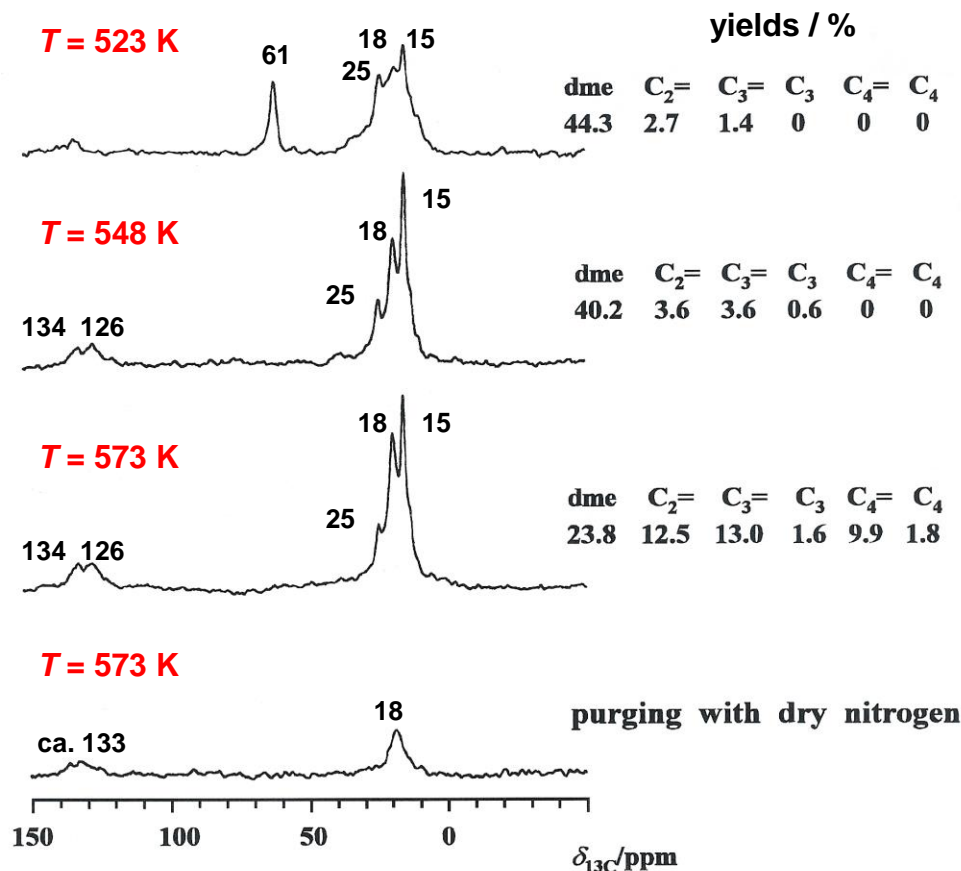
## II: Steady-state conditions

MAS NMR technique for the study of hydrocarbon-pool compounds under *in situ* conditions



## II: Steady-state conditions

*in situ*  $^{13}\text{C}$  MAS NMR study of the hydrocarbon pool formation on H-ZSM-5 during methanol conversion with  $\text{WHSV} = 1.25 \text{ h}^{-1}$



$T < 523 \text{ K:}$

mixture of olefinic and aromatic compounds, such as:

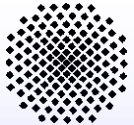
3-hexene (14.4, 25.9, 131.2 ppm)  
2,4-hexadiene (17.2, 126.2, 132.5 ppm)  
....

hexamethylbenzene (17.6, 132.1 ppm)

$T > 573 \text{ K:}$

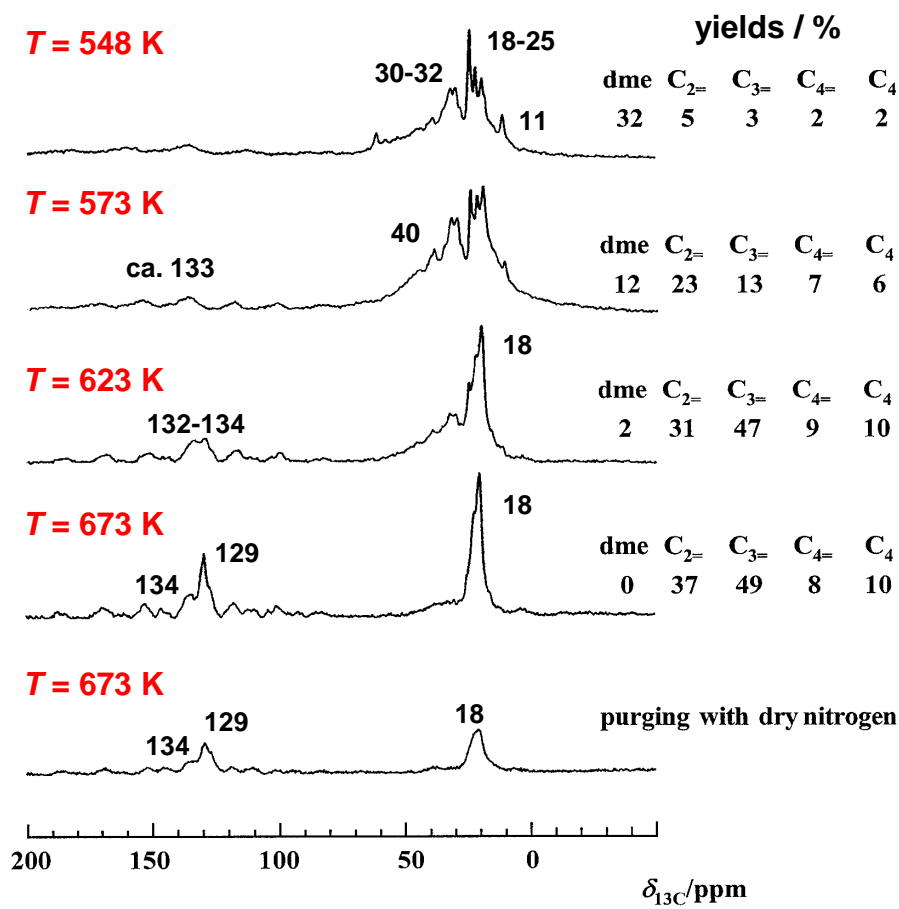
polymethylaromatics remain after purging, such as:

toluene (20.3, 128.5, 129.0 ppm)  
....  
hexamethylbenzene (17.6, 132.1 ppm)



## II: Steady-state conditions

*in situ*  $^{13}\text{C}$  MAS NMR study of the hydrocarbon pool formation on SAPO-34 during methanol conversion with  $\text{WHSV} = 1.25 \text{ h}^{-1}$



$T < 573 \text{ K}$ :

mixture of olefinic and aromatic compounds, such as:

2-methyl-2-butene (9.3-22.5, 118.8, 131.8 ppm)  
2,4-hexadiene (19.5, 132.5 ppm)

....  
tetramethylbenzene (18.9, 131.1, 134.0 ppm)

$T > 623 \text{ K}$ :

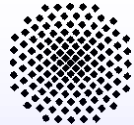
domination of polymethyl-aromatics, such as:

toluene (20.3, 128.5, 129.0 ppm)

....

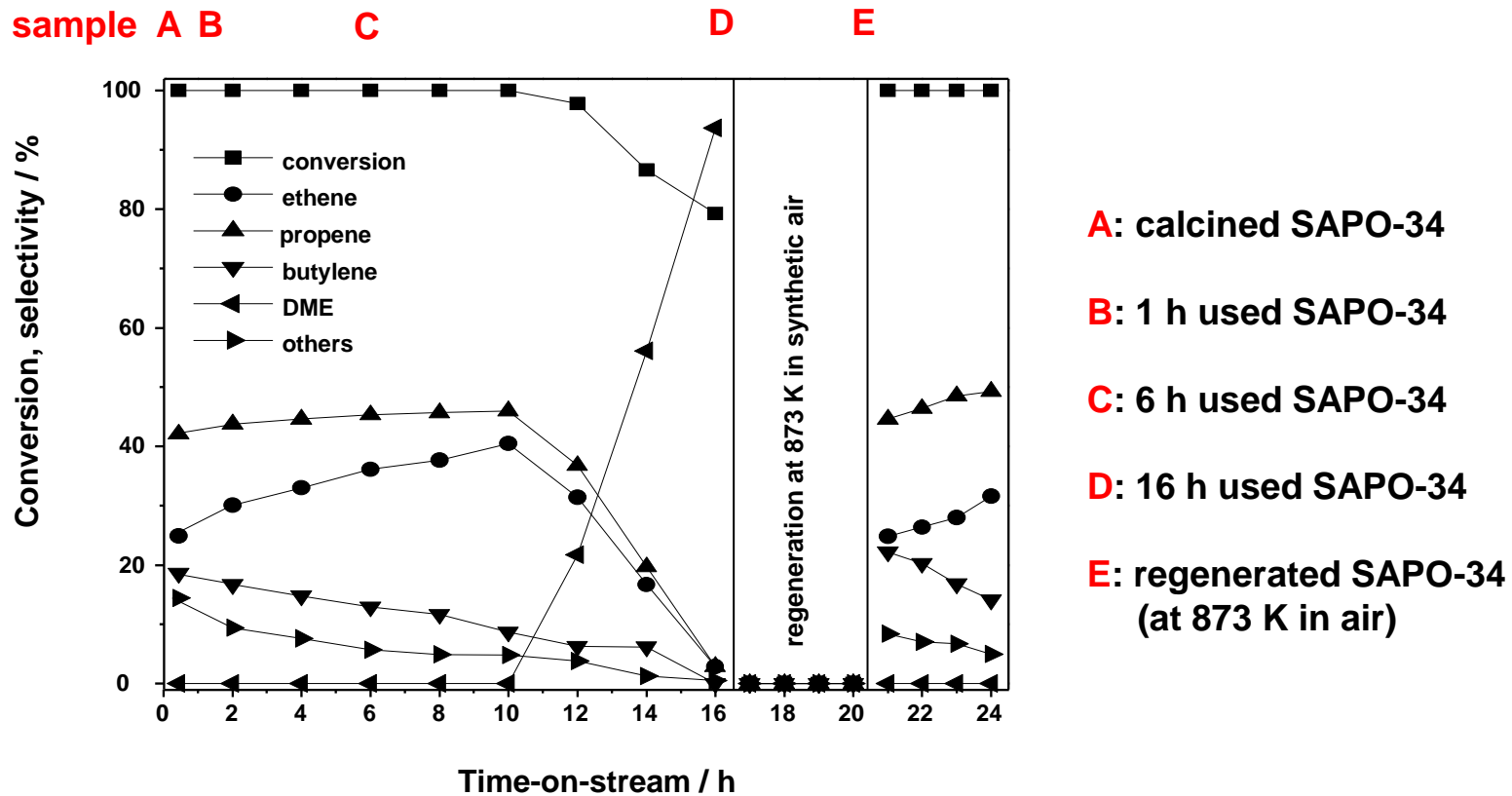
trimethylbenzene (21.2, 127.4, 137.6 ppm)

hexamethylbenzene (17.6, 132.1 ppm)



## II: Steady-state conditions

preparation of SAPO-34 catalysts (**B**, **C**, and **D**) loaded with hydrocarbon-pool compounds by MTO conversion in a fixed-bed reactor at  $T = 673\text{ K}$  ( $\text{WHSV} = 0.5\text{ h}^{-1}$ )

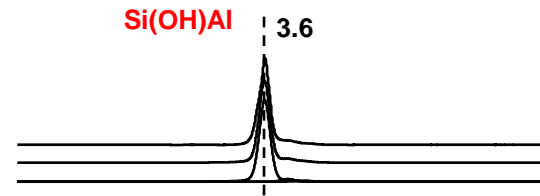


## II: Steady-state conditions

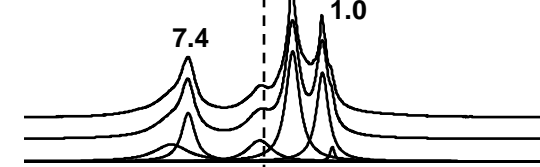
**$^1\text{H}$  MAS NMR studies of SAPO-34 catalysts obtained upon MTO conversion in a fixed-bed reactor at 673 K ( $\text{WHSV} = 0.5 \text{ h}^{-1}$ )**

$^1\text{H}$  MAS NMR spectra recorded with  $\nu_{\text{rot}} = 25 \text{ kHz}$

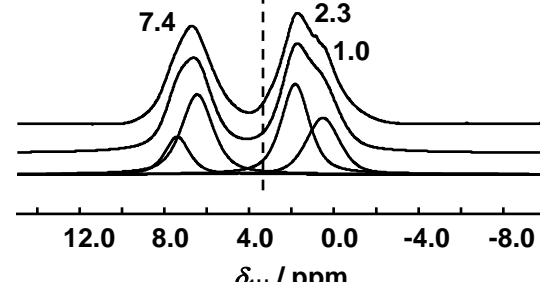
calcined SAPO-34 (A)



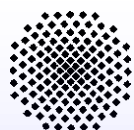
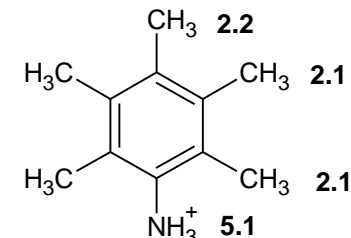
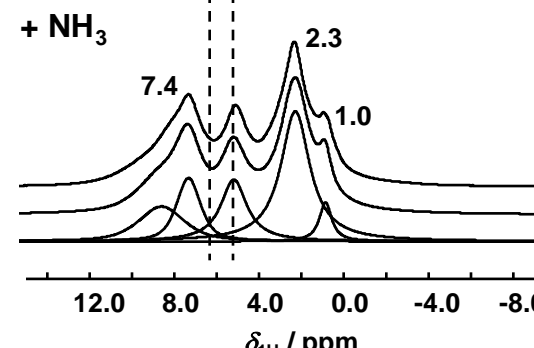
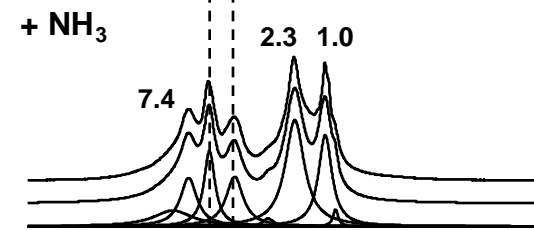
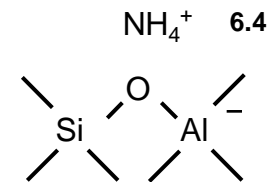
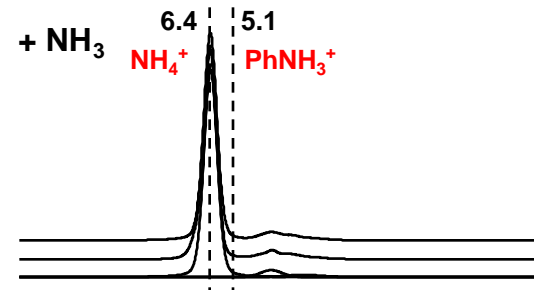
1 h used SAPO-34 (B)

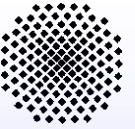


6 h used SAPO-34 (C)



$^1\text{H}$  NMR shifts / ppm:





## II: Steady-state conditions

numbers of bridging OH groups,  $n_{\text{SiOHAl}}$ , ammonium,  $n_{\text{NH}_4^+}$ , and polyalkylphenyl-ammonium ions,  $n_{\text{PhNH}_3^+}$ , formed upon loading of ammonia on SAPO-34 catalysts

catalyst samples	$n_{\text{SiOHAl}}^{*)}$	$n_{\text{NH}_4^+}^{*)}$	$n_{\text{PhNH}_3^+}^{*)}$
calcined SAPO-34 ( <b>A</b> )	1.45 mmol/g	-	-
calcined SAPO-34 ( <b>A</b> ) + NH <sub>3</sub>	0.15 mmol/g	1.30 mmol/g	0
1 h used SAPO-34 ( <b>B</b> )	0.56 mmol/g	-	-
1 h used SAPO-34 ( <b>B</b> ) + NH <sub>3</sub>	0.13 mmol/g	0.33 mmol/g	0.40 mmol/g
6 h used SAPO-34 ( <b>C</b> )	0	-	-
6 h used SAPO-34 ( <b>C</b> ) + NH <sub>3</sub>	0	0	0.82 mmol/g

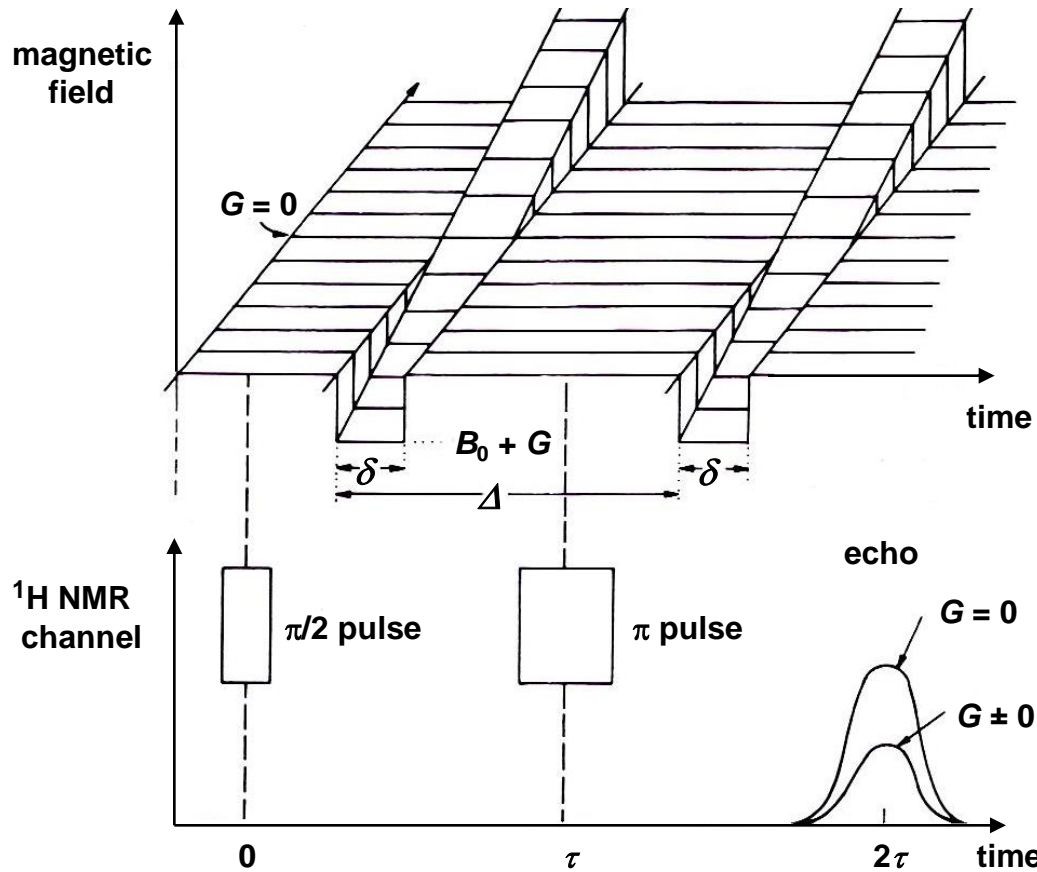
\*) accuracy of  $\pm 10\%$  for the numbers,  $n_i$ , determined by <sup>1</sup>H MAS NMR spectroscopy



## II: Steady-state conditions

self-diffusivity  $D$  of reactants in MTH catalysts

pulsed-field gradient NMR experiment (PFG NMR)



evaluation:

$$A(G)/A(0) = \exp \{-\gamma^2 G^2 \delta^2 \Delta D\}$$

gyromagnetic ratio      /      /  
gradient strength      |  
gradient delay  
gradient duration

accessible range:

$$D = 10^{-10} \dots 10^{-13} \text{ m}^2/\text{s}$$

upper limit:

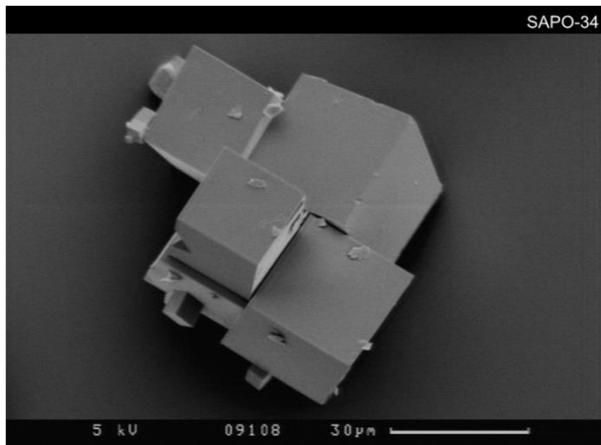
$$D = r_c^2 / 6 \Delta$$

|  
crystal radius

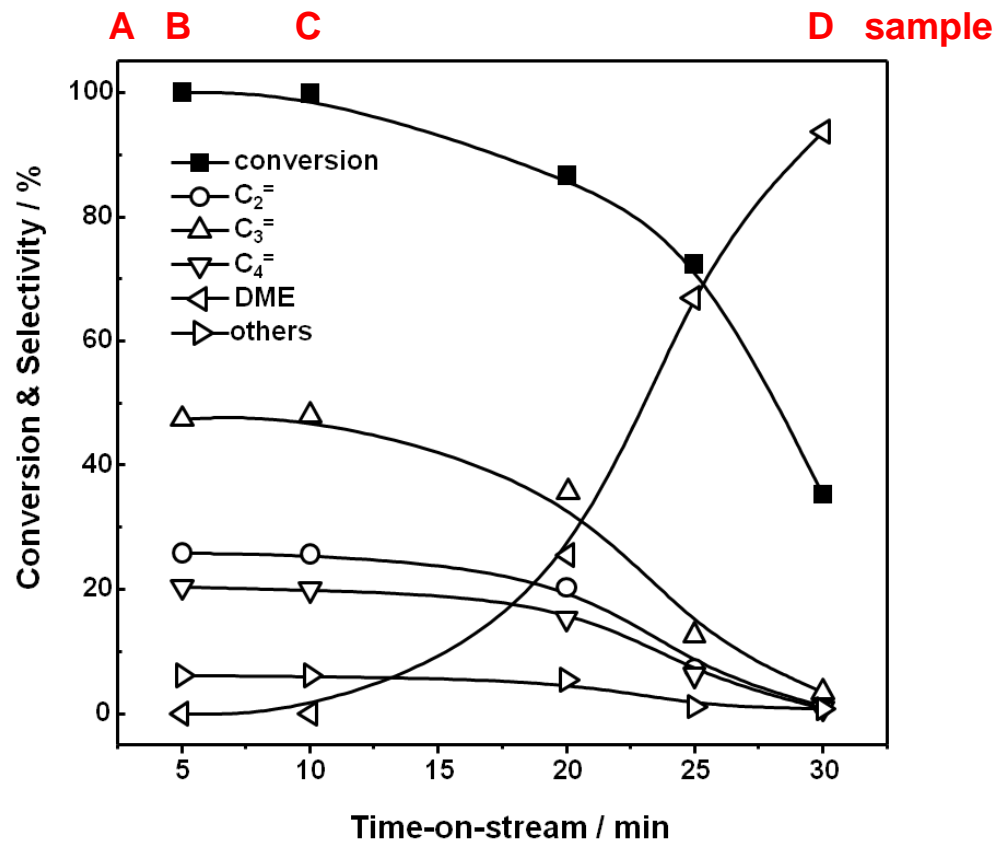
## II: Steady-state conditions

self-diffusivity  $D$  of reactants in the MTH catalyst SAPO-34

SEM picture of large-crystalline SAPO-34



MTH conversion on large-crystalline SAPO-34 at 643 K with  $WHSV = 1 \text{ h}^{-1}$



SAPO-34 under study:

$$n_{\text{Si}}/(n_{\text{Al}}+n_{\text{P}}+n_{\text{Si}}) = 0.15$$

sizes of 20 to 30  $\mu\text{m}$



## II: Steady-state conditions

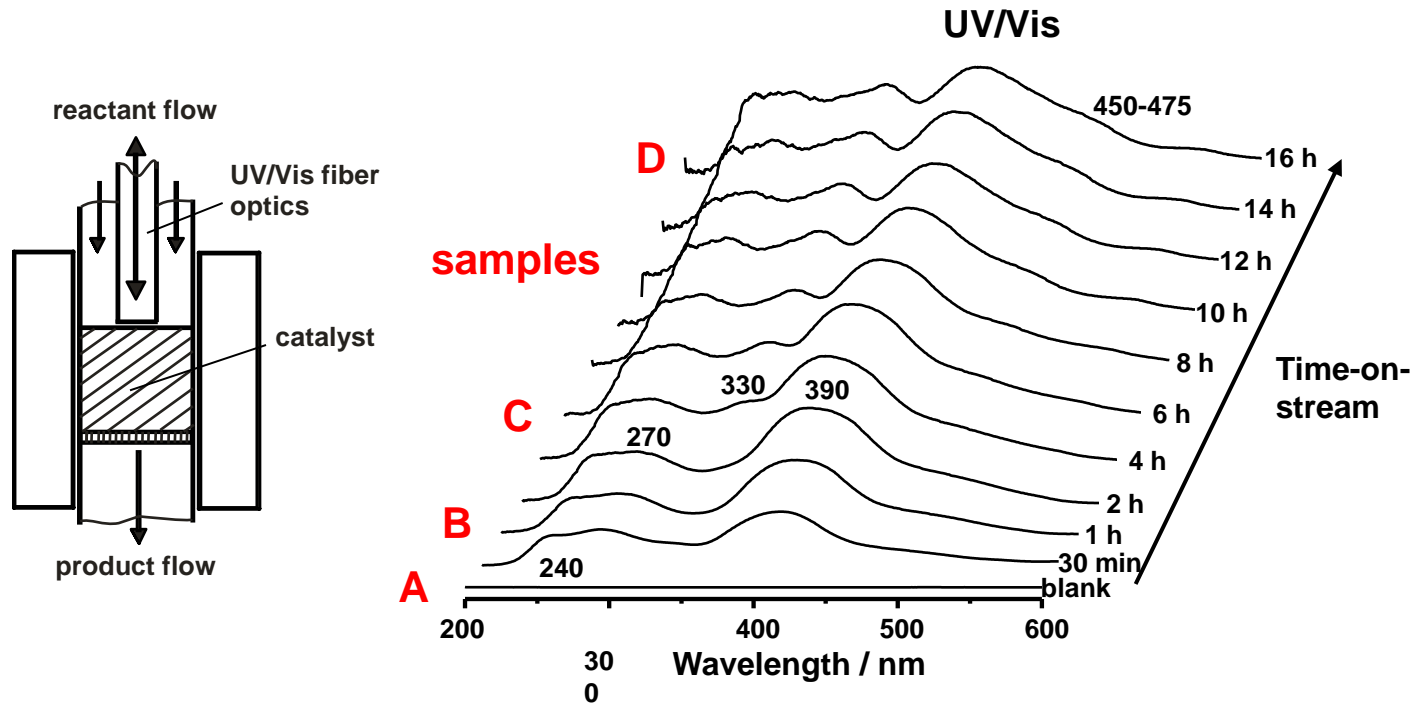
self-diffusivity  $D$  of reactants in the MTH catalyst SAPO-34

loading / cage	$D / \text{m}^2\text{s}^{-1}$			
	sample A $TOS = 0 \text{ min}$	sample B $TOS = 5 \text{ min}$	sample C $TOS = 10 \text{ min}$	sample D $TOS = 30 \text{ min}$
1 ethene	$1.3 \times 10^{-11}$	$8.0 \times 10^{-12}$	$7.7 \times 10^{-12}$	$5.8 \times 10^{-12}$
1 ethane	$6.7 \times 10^{-12}$	$4.9 \times 10^{-12}$	$2.4 \times 10^{-12}$	$2.2 \times 10^{-12}$
2 ethene	$1.3 \times 10^{-11}$	$9.2 \times 10^{-12}$	$8.7 \times 10^{-12}$	-
2 ethane	$5.7 \times 10^{-12}$	$4.4 \times 10^{-12}$	$2.3 \times 10^{-12}$	-
3 ethene	$1.6 \times 10^{-11}$	$1.1 \times 10^{-11}$	$9.9 \times 10^{-12}$	-
3 ethane	$4.4 \times 10^{-12}$	$4.1 \times 10^{-12}$	$2.3 \times 10^{-12}$	-

diffusion selectivity  $D_{\text{ethene}} / D_{\text{ethane}}$  increases from ca. 1.6 for catalysts with small TOS and low adsorbate loading to 3.8 for catalysts with long TOS and high adsorbate loading

## II: Steady-state conditions

UV/Vis studies of SAPO-34 catalysts during MTO conversion in a fixed-bed reactor at 673 K ( $WHSV = 0.5 \text{ h}^{-1}$ )



assignment of UV/Vis bands:

240 nm: dienes

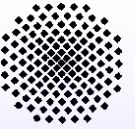
270 nm: aromatics and polyalkylaromatics

330 nm: cyclohexadienyl carbenium ion

390 nm: benzene-type carbenium ions

450 nm: trienylic carbenium ions

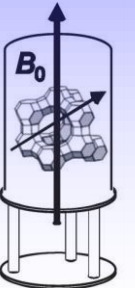
400-475 nm: polycyclic aromatics



## ***II: Steady-state conditions***

**assignments of UV/Vis bands ( $\pi\text{-}\pi^*$  transitions) observed during the methanol-to-olefin conversion on acidic zeolite catalysts**

<b>Bands at <math>\lambda / \text{nm}</math></b>	<b>Assignments</b>
240	dienes
270	aromatics and polyalkyl aromatics
320	monoenyl carbenium ions
330	cyclohexadienyl carbenium ions
390	benzenium-type carbenium ions
400-475	polycyclic aromatics
450	triénylic carbenium ions



### **References:**

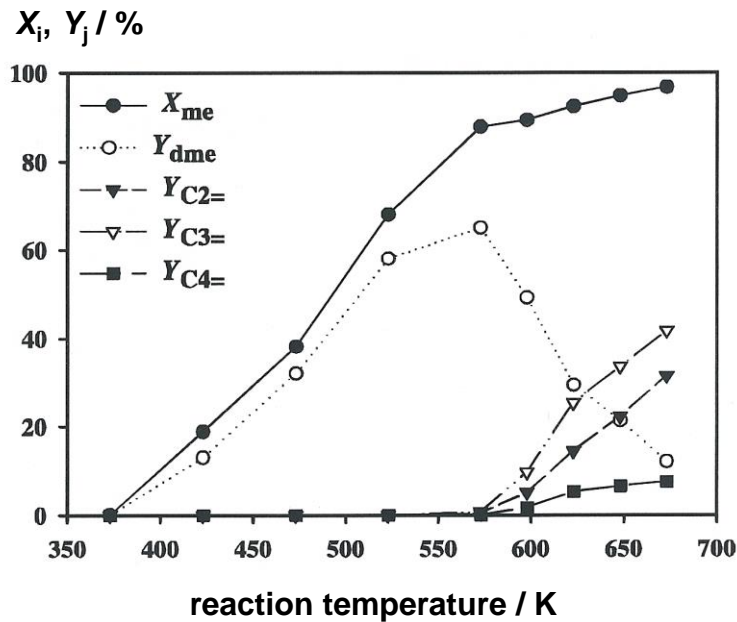
- H.G. Karge et al., Stud. Surf. Sci. Catal. 49 (1989) 1327.
- I. Kirisci et al., Chem. Rev. 99 (1999) 2085.
- H. Foerster et al., J. Mol. Struct. 296 (1993) 61.
- M. Bjørgen et al., J. Am. Chem. Soc. 125 (2003) 15863.

## II: Steady-state conditions

comparison of MTH on H-ZSM-5 in standard fixed bed and rotor reactors,  
A. Buchholz, diploma thesis, University Stuttgart, 2000

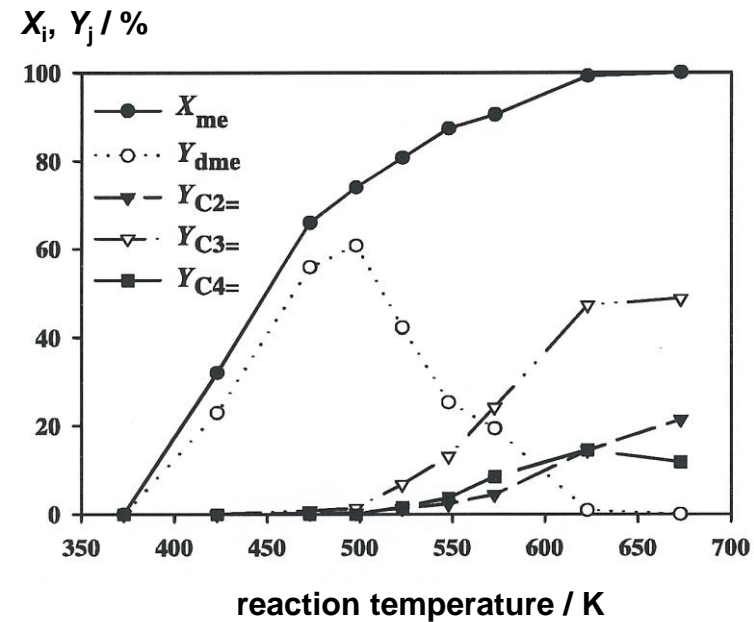
fixed-bed reactor

WHSV = 1.25 h<sup>-1</sup>



spinning (2 kHz) MAS NMR rotor

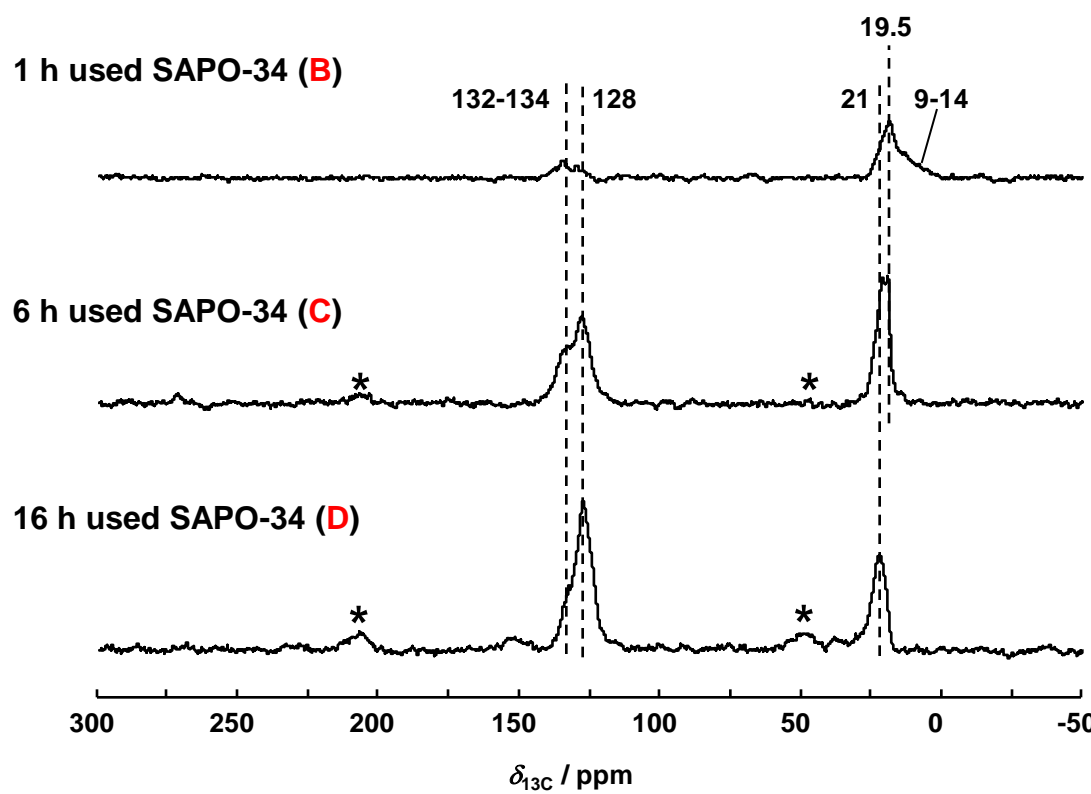
WHSV = 1.25 h<sup>-1</sup>



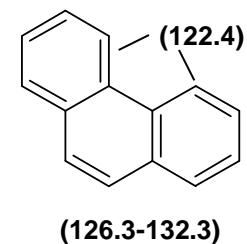
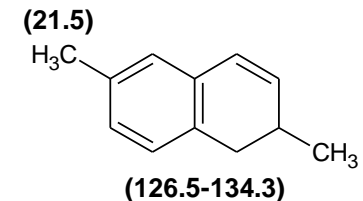
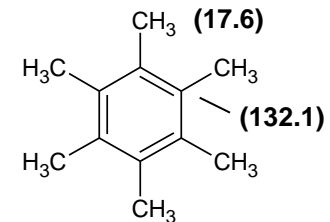
## II: Steady-state conditions

**$^{13}\text{C}$  MAS NMR studies of SAPO-34 catalysts obtained upon MTO conversion in a fixed-bed reactor at 673 K ( $\text{WHSV} = 0.5 \text{ h}^{-1}$ )**

$^{13}\text{C}$  MAS NMR spectra



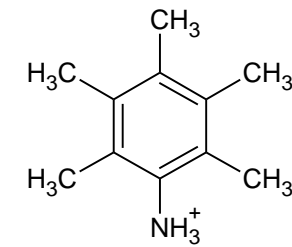
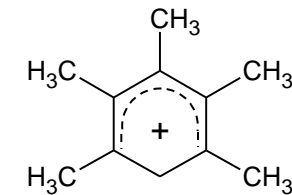
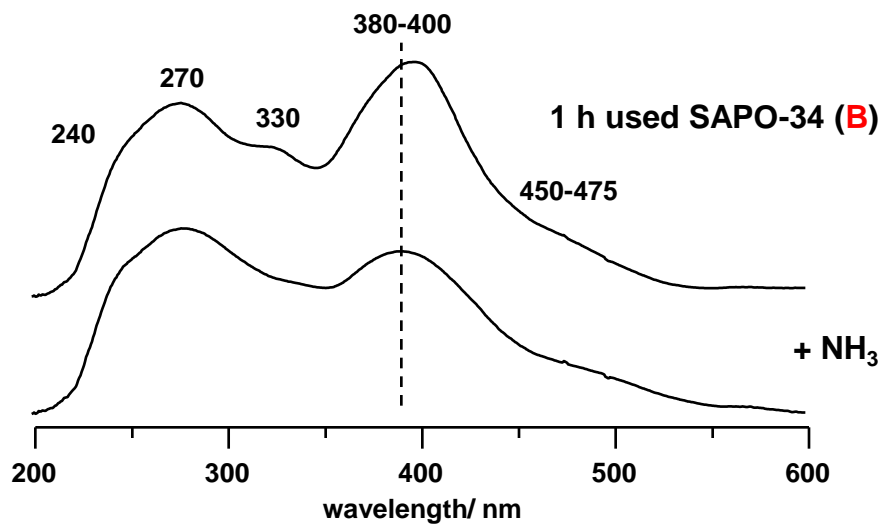
$^{13}\text{C}$  NMR shifts / ppm:



## II: Steady-state conditions

UV/Vis spectra of SAPO-34 used as MTO catalyst for 1 h (sample B) and recorded before and after ammonia loading

UV/Vis



assignment of UV/Vis bands:

240 nm: dienes

270 nm: aromatics and polyalkylaromatics

330 nm: cyclohexadienyl carbenium ion

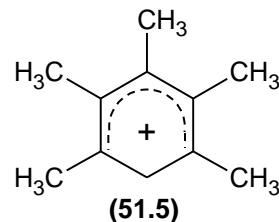
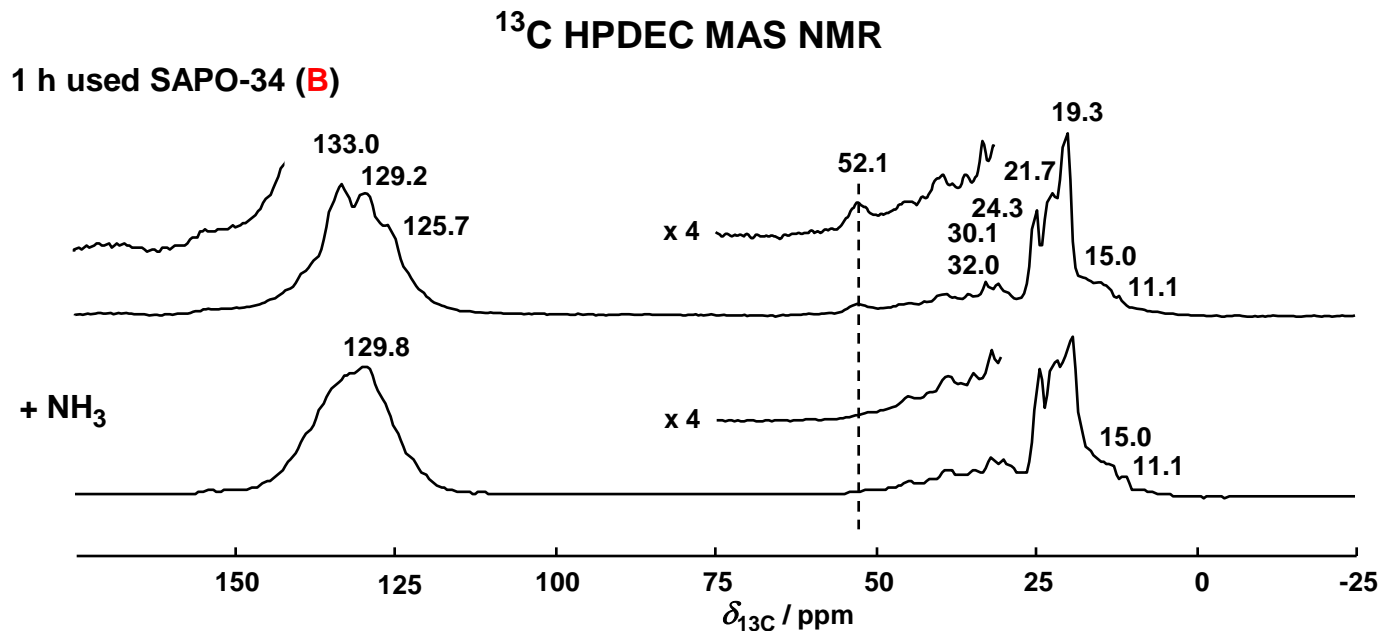
390 nm: benzene-type carbenium ions

450 nm: trienylic carbenium ions

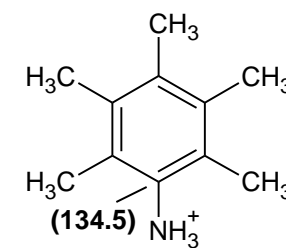
400-475 nm: polycyclic aromatics

## II: Steady-state conditions

<sup>13</sup>C HPDEC MAS NMR spectra of SAPO-34 used as MTO catalyst for 1 h (sample B) and recorded before and after ammonia loading

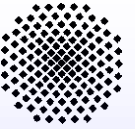


$(\delta_{13\text{C}} = 16.1-17.5; 51.5; 131.9-134.6 \text{ ppm})$



$(\delta_{13\text{C}} = 13.6-17.6; 129.8-134.6 \text{ ppm})$



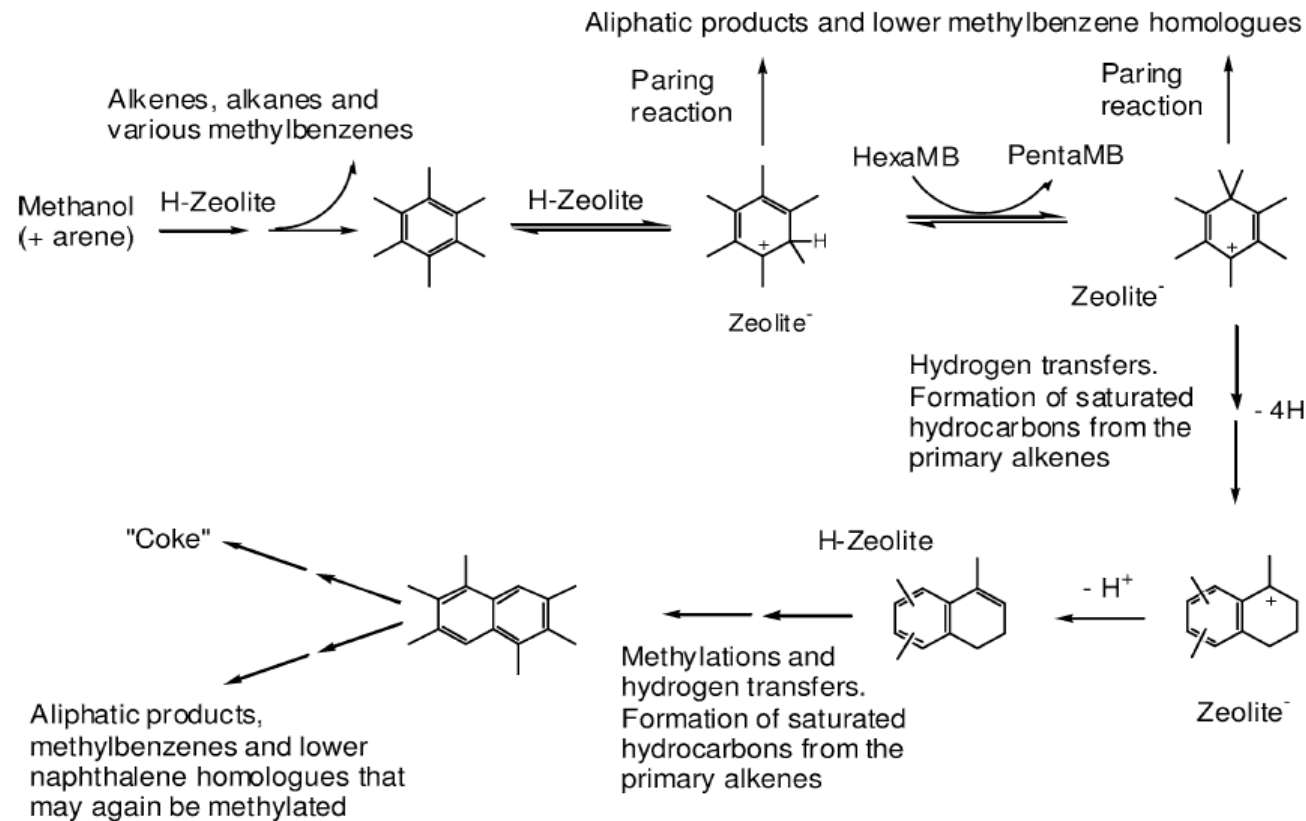


### *III. Deactivation of MTO catalysts by coke formation*



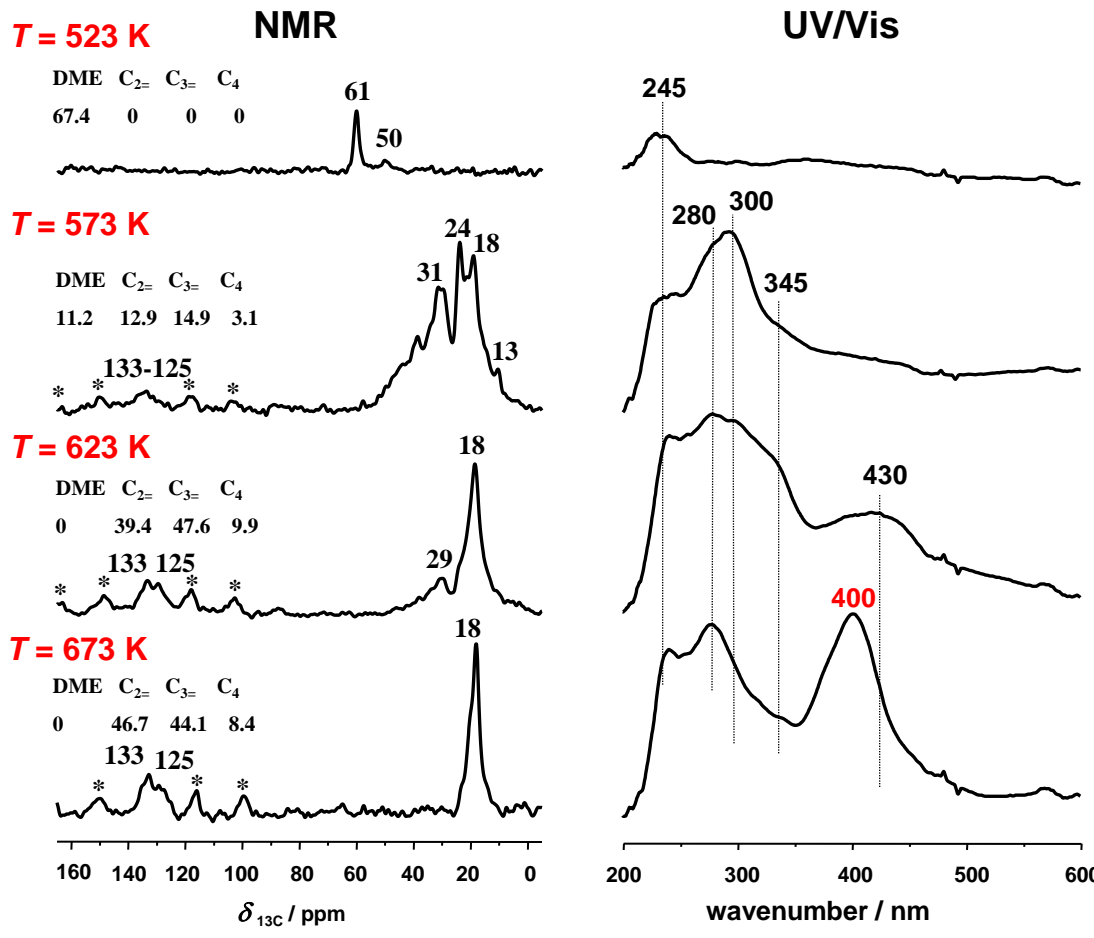
### III: Catalyst deactivation

mechanism of coke formation in SAPO-34 catalysts by sequential conversion of hexamethylbenzene (M. Bjorgen et al., J. Catal. 215 (2003) 30)



### III: Catalyst deactivation

*in situ*  $^{13}\text{C}$  MAS NMR-UV/Vis spectroscopy of coke formation on H-SAPO-34 at 523 to 673 K for 3 h under continuous-flow conditions



#### NMR:

- quantitative evaluation
- separation of alkyl groups and aromatics
- rotor reactor comparable with fixed-bed reactor

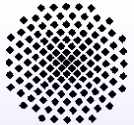
#### UV/Vis:

- sensitive for carbenium cations
- separation of aromatics and polycyclic aromatics

Y. Jiang et al., Microporous Mesoporous Mater. 105 (2007) 132.

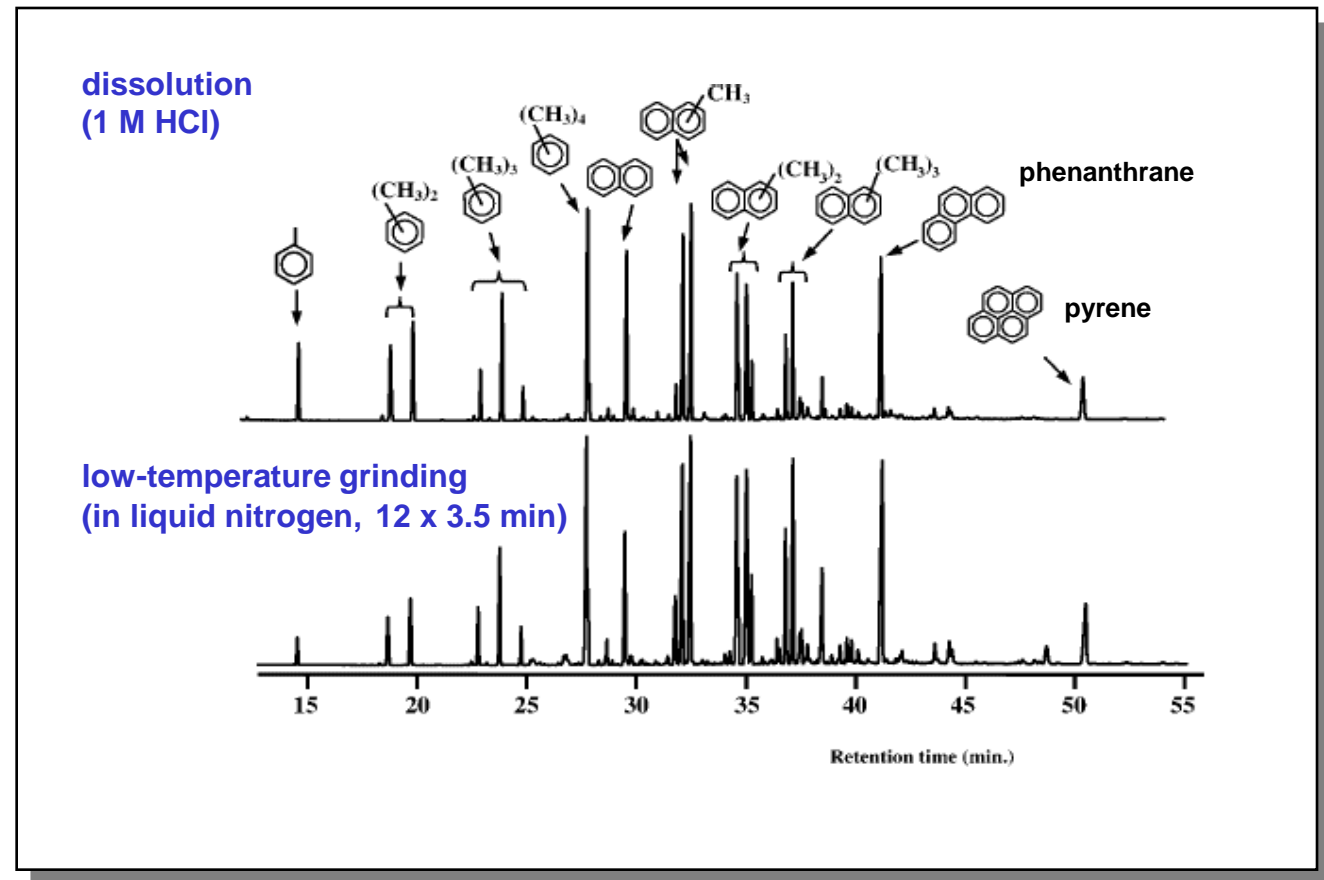
400-475 nm: polycyclic aromatics

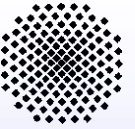
400 nm: polymethylanthracenes



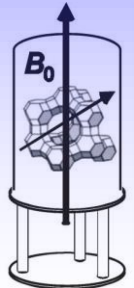
### III: Catalyst deactivation

*ex situ* study of coke deposits via dissolution and low-temperature grinding of used SAPO-34 catalysts (H. Fu et al., Catal. Lett. 76 (2001) 89)



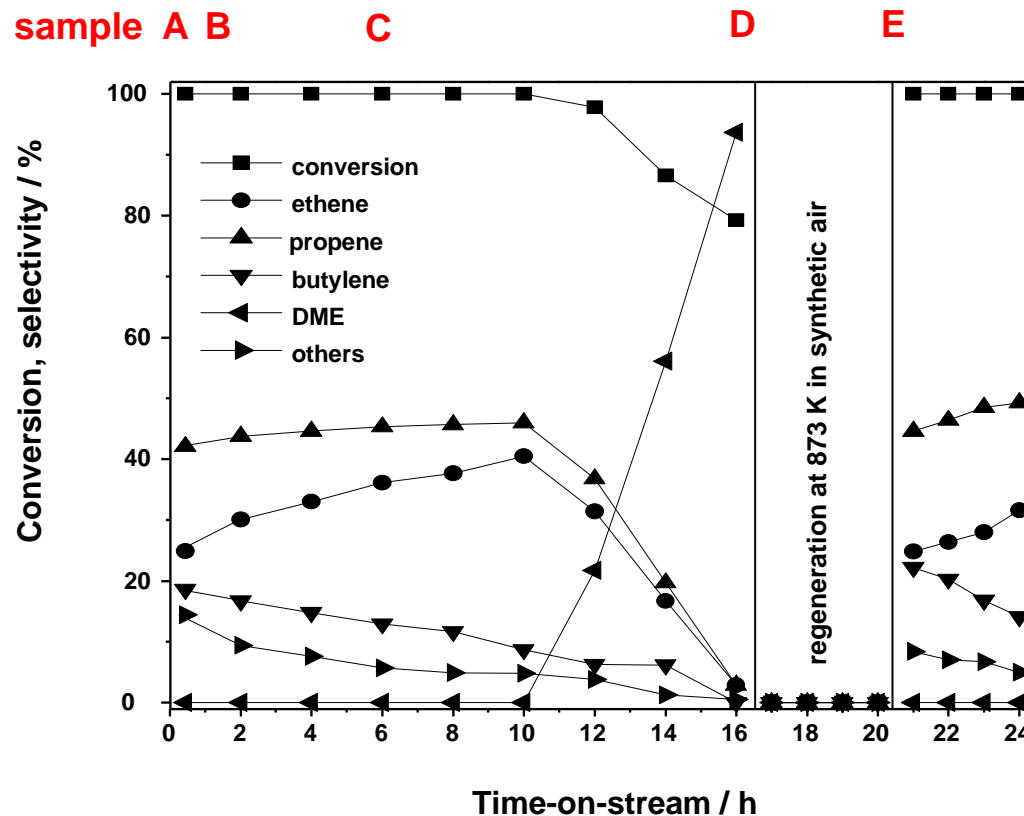


## *IV. Catalyst regeneration*



## IV: Catalyst regeneration

regeneration of SAPO-34 catalysts (D) in synthetic air at 873 K for 4 h leading to sample E



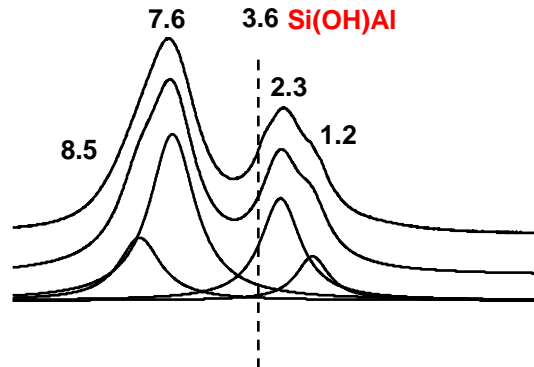
- A: calcined SAPO-34
- B: 1 h used SAPO-34
- C: 6 h used SAPO-34
- D: 16 h used SAPO-34
- E: regenerated SAPO-34 (at 873 K in air)

## IV: Catalyst regeneration

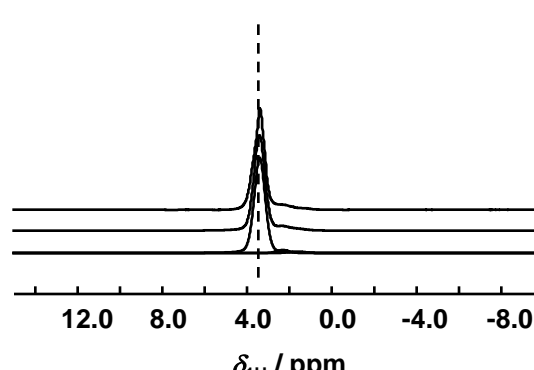
<sup>1</sup>H MAS NMR studies of SAPO-34 catalysts obtained upon MTO conversion in a fixed-bed reactor at 673 K for 16 h (D) and after regeneration at 873 K in air (E)

<sup>1</sup>H MAS NMR spectra recorded with  $\nu_{\text{rot}} = 25 \text{ kHz}$

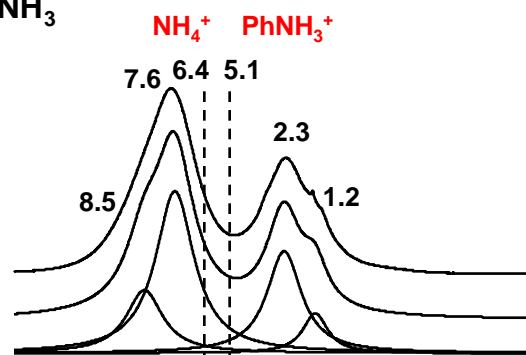
16 h used SAPO-34 (D)



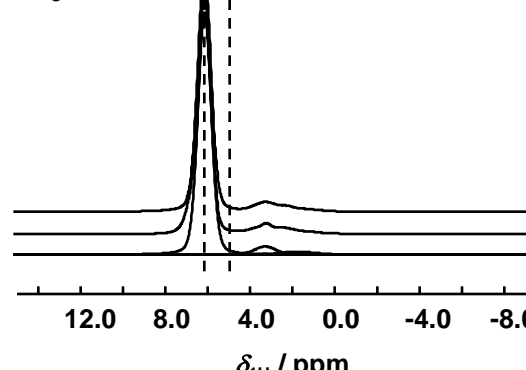
regenerated SAPO-34 (E)



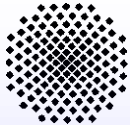
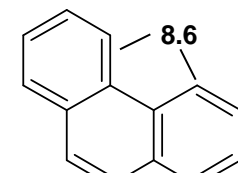
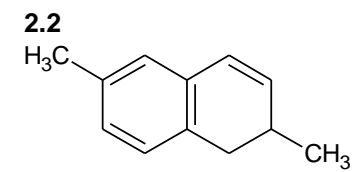
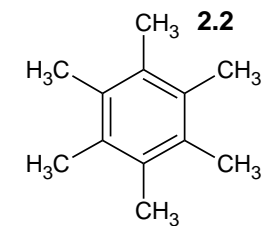
+ NH<sub>3</sub>



+ NH<sub>3</sub>



<sup>1</sup>H NMR shifts / ppm:

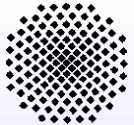


## IV: Catalyst regeneration

numbers of bridging OH groups,  $n_{\text{SiOHAl}}$ , ammonium,  $n_{\text{NH}_4^+}$ , and polyalkylphenylammonium ions,  $n_{\text{PhNH}_3^+}$ , formed upon loading of ammonia on the calcined (**A**), used (**D**), and regenerated SAPO-34 catalysts (**E**)

catalyst samples	$n_{\text{SiOHAl}}^{*)}$	$n_{\text{NH}_4^+}^{*)}$	$n_{\text{PhNH}_3^+}^{*)}$
calcined SAPO-34 ( <b>A</b> )	1.45 mmol/g	-	-
calcined SAPO-34 ( <b>A</b> ) + NH <sub>3</sub>	0.15 mmol/g	1.30 mmol/g	0
16 h used SAPO-34 ( <b>D</b> )	0	-	-
16 h used SAPO-34 ( <b>D</b> ) + NH <sub>3</sub>	0	0	0
regenerated SAPO-34 ( <b>E</b> )	1.25 mmol/g	-	-
regenerated SAPO-34 ( <b>E</b> ) + NH <sub>3</sub>	0.10 mmol/g	1.15 mmol/g	0

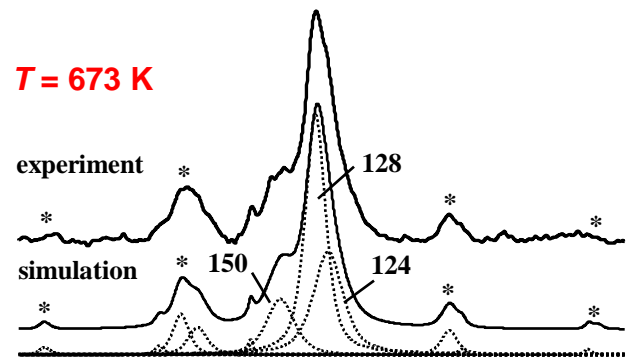
\*) accuracy of  $\pm 10\%$  for the numbers,  $n_i$ , determined by <sup>1</sup>H MAS NMR spectroscopy



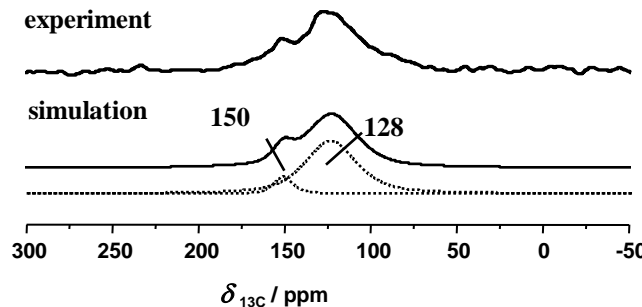
## IV: Catalyst regeneration

regeneration of coked H-SAPO-34 (like sample D) by purging with synthetic air (20 vol.-% O<sub>2</sub>, 30 ml/min) at T = 673 and 773 K for 2 h

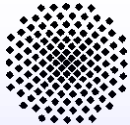
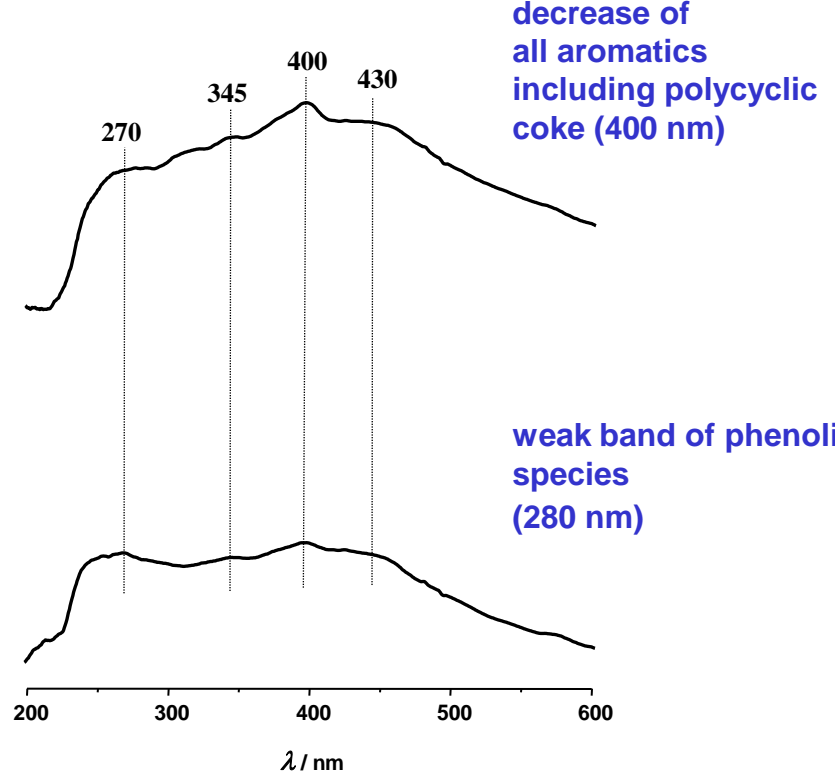
<sup>13</sup>C MAS NMR

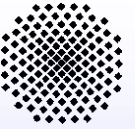


T = 773 K



UV/Vis

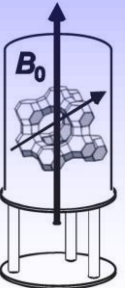




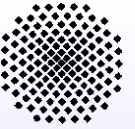
## IV: Catalyst regeneration

evaluation of the  $^{13}\text{C}$  MAS NMR spectra of coked SAPO-34 (like sample D) before and after regeneration in synthetic air for 2 h

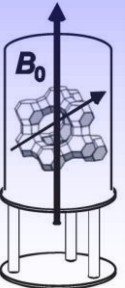
signal at $\delta_{^{13}\text{C}}$ / ppm	assignments	number of $^{13}\text{C}$ atoms in mmol / g		
		reaction at 673 K	syn. air at 673 K	syn. air at 773 K
16-21	carbon in methyl groups bound to aromatics	0.53	-	-
14-15 and 22-29	carbon in ethyl groups bound to aromatics	0.16	-	-
125-137	carbon in alkylated and nonalkylated aromatic rings	3.33	0.17	0.05
145-155	carbon in aromatics bound to oxygen atoms	-	0.45	0.13

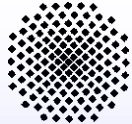


thermal destruction of all aromatics (UV/Vis bands at 280 nm and 400 nm), but formation of oxygenated species (270 nm)



## *V. Recent approaches for improved MTP catalysts*

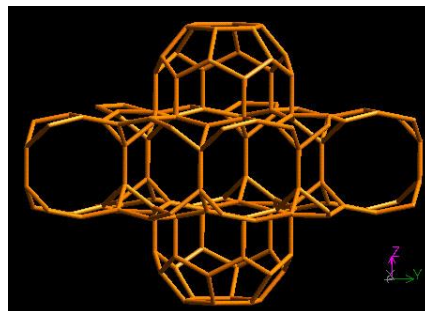




## V: Recent approaches for improved MTP catalysts

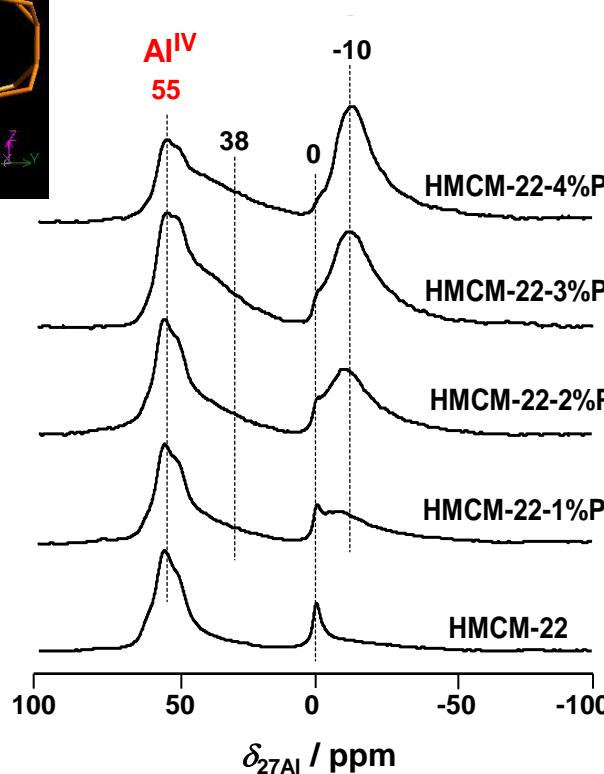
modification of MCM-22 ( $n_{\text{Si}}/n_{\text{Al}} = 15$ ) with 0.5 M  $(\text{NH}_4)_2\text{HPO}_4$  (X. Wang, W. Dai, G. Wu, L. Li, N. Guan, M. Hunger, Microporous Mesoporous Mater. 151 (2012) 99)

structure type MWW:

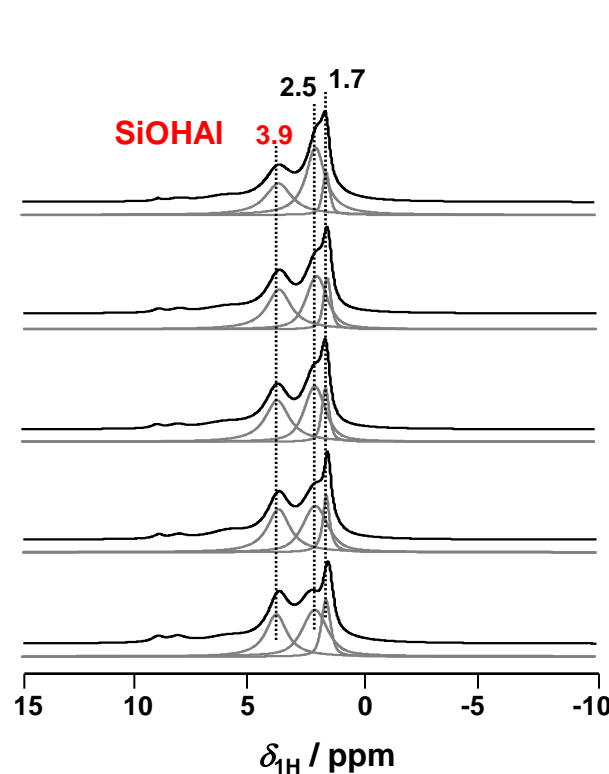


10-ring pores with sizes of 0.40 nm x 0.55 nm  
and 0.41 nm x 0.51 nm

$^{27}\text{Al}$  MAS NMR



$^1\text{H}$  MAS NMR



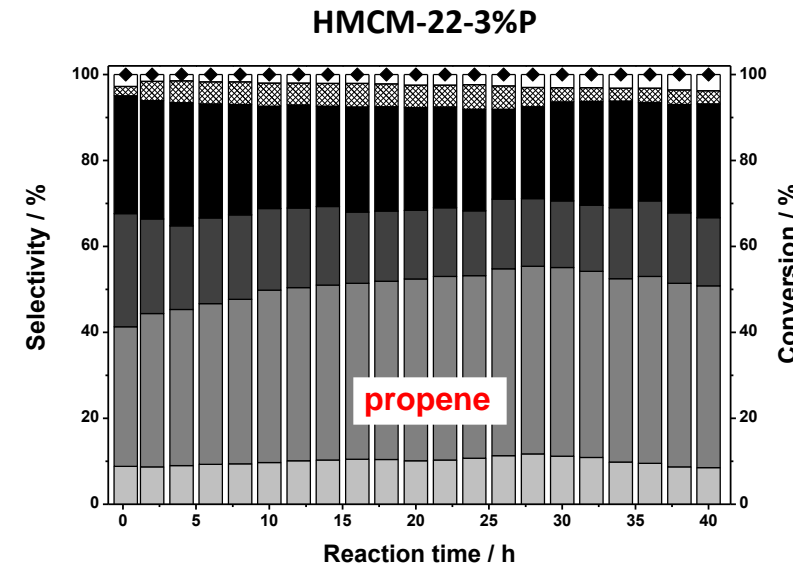
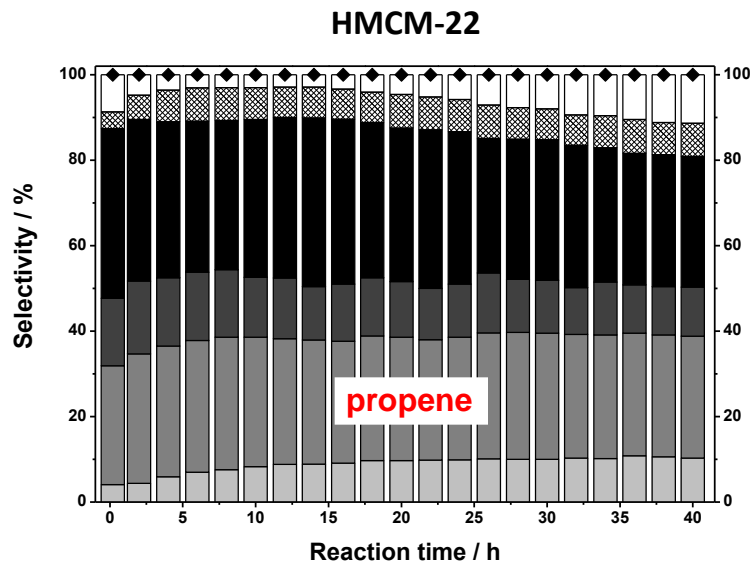
MWW cage



## V: Recent approaches for improved MTP catalysts

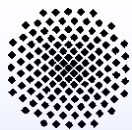
modification of MCM-22 ( $n_{\text{Si}}/n_{\text{Al}} = 15$ ) with 0.5 M  $(\text{NH}_4)_2\text{HPO}_4$  (X. Wang, W. Dai, G. Wu, L. Li, N. Guan, M. Hunger, Microporous Mesoporous Mater. 151 (2012) 99)

methanol conversion at 723 K with  $\text{WHSV} = 1 \text{ h}^{-1}$



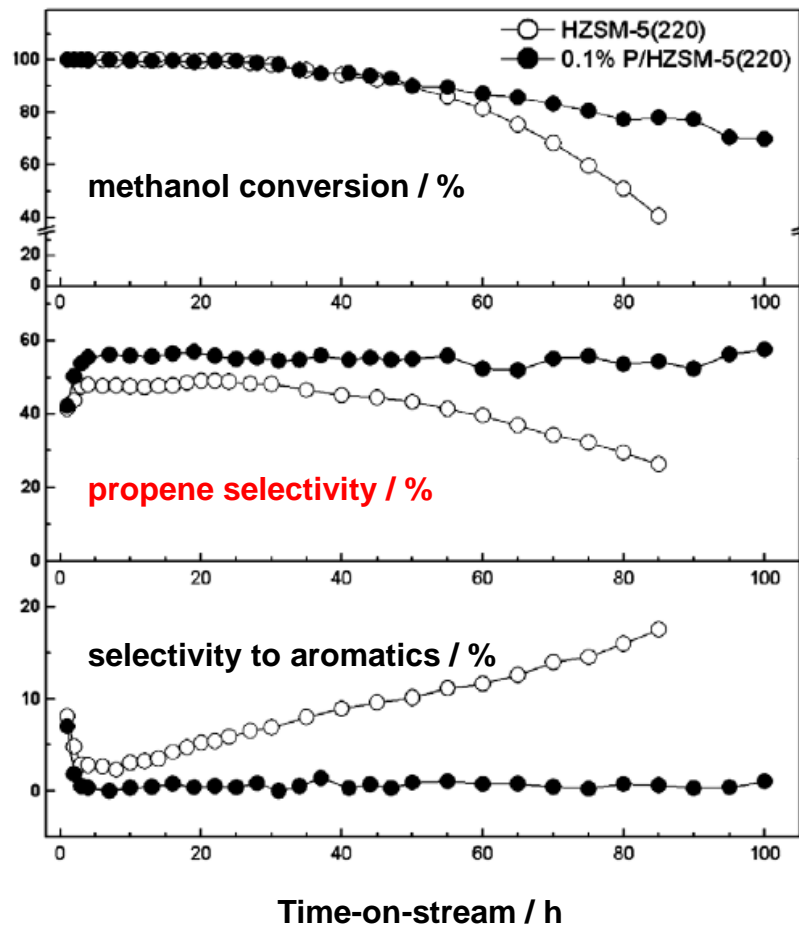
CH <sub>4</sub>
Aromatics
Paraffins
C <sub>2</sub> H <sub>6</sub>
C <sub>3</sub> H <sub>6</sub>
C <sub>2</sub> H <sub>4</sub>

- maximum propene selectivity observed for MCM-22 with 3 wt% phosphorus
- significant dealumination of the framework and decrease of the number of strong acid sites



## V: Recent approaches for improved MTP catalysts

modification of high-silica ZSM-5 ( $n_{\text{Si}}/n_{\text{Al}} = 220$ ) by impregnation with a desired amount (0.1 wt%) of  $\text{H}_3\text{PO}_4$  (J. Liu, C. Zhang, Z. Shen, W. Hua, Y. Tang, W. Shen, Y. Yue, H. Xu, Catal. Commun. 10 (2009) 1506)



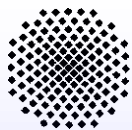
textural properties of parent and P-modified high-silica ZSM-5:

Catalyst	$A_{\text{BET}}$ ( $\text{m}^2/\text{g}$ )	$A_L$ ( $\text{m}^2/\text{g}$ )	$A_M$ ( $\text{m}^2/\text{g}$ )	$V_M$ ( $\text{cm}^3/\text{g}$ )	$V_T$ ( $\text{cm}^3/\text{g}$ )
HZSM-5(220)	376	470	349	0.160	0.248
0.1%P/HZSM-5(220)	367	461	336	0.155	0.273

methanol ( $\text{MeOH:H}_2\text{O} = 1:5$ ) conversion at 733 K with  $LHSV = 0.75 \text{ h}^{-1}$ :

- enhancement of propene selectivity from 46.4 % to 55.5 % is explained by partial elimination of strong Broensted acid sites due to  $\text{H}_3\text{PO}_4$  treatment

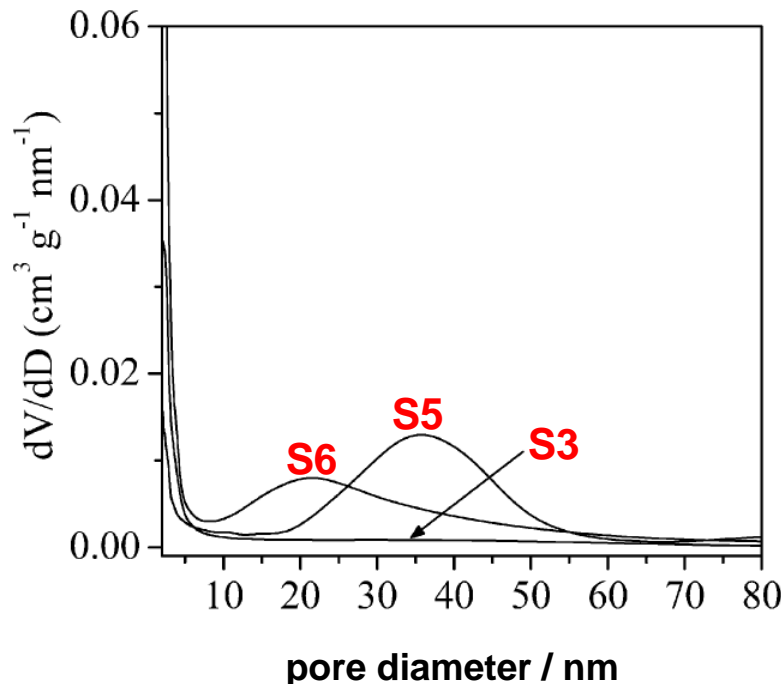




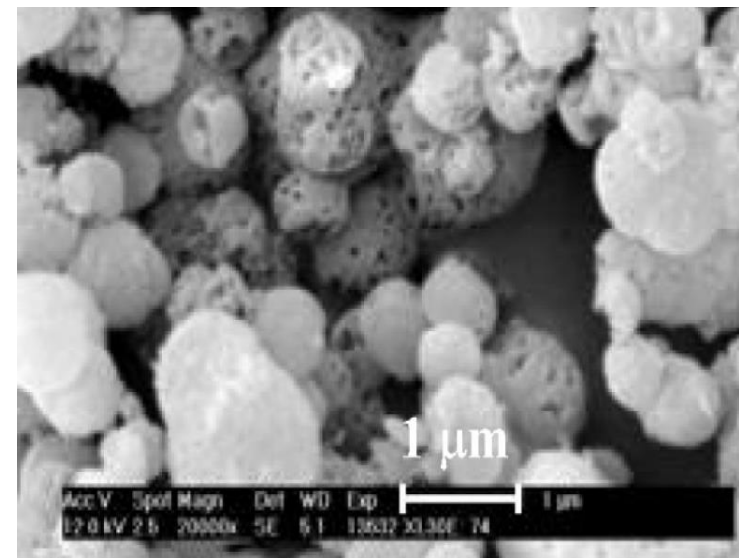
## V: Recent approaches for improved MTP catalysts

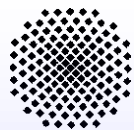
modification of high-silica ZSM-5 (**S3**:  $n_{\text{Si}}/n_{\text{Al}} = 72$ ) by treatment with 0.45 M  $\text{Na}_2\text{CO}_3$  and 1 M HCl (**S5**:  $n_{\text{Si}}/n_{\text{Al}} = 78$ ) and addition of starch to the synthesis gel (**S6**:  $n_{\text{Si}}/n_{\text{Al}} = 76$ ) (C. Mei, P. Wen, Z. Liu, Y. Wang, W. Yang, Z. Xie, W. Hua, Z. Gao, J. Catal. 258 (2008) 243)

pore size distribution



SEM picture of sample **S5**

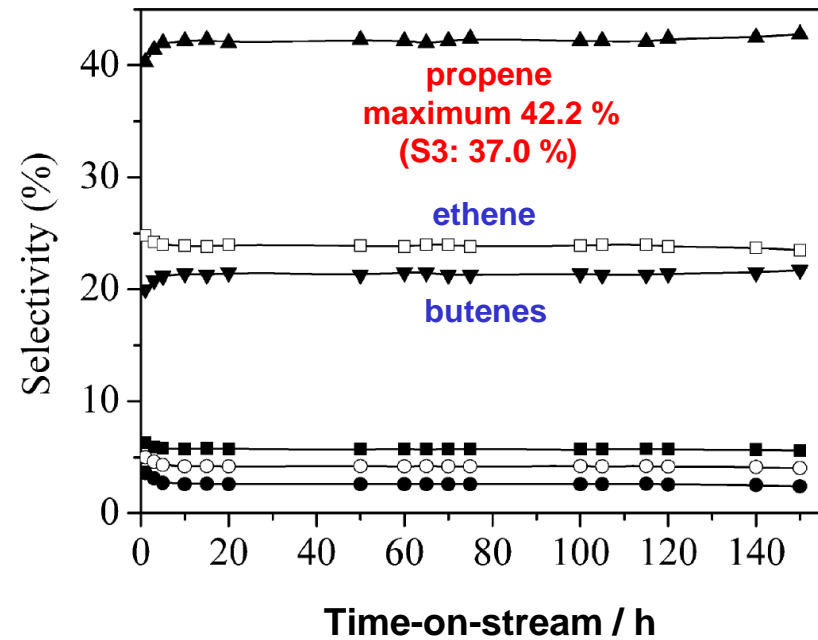
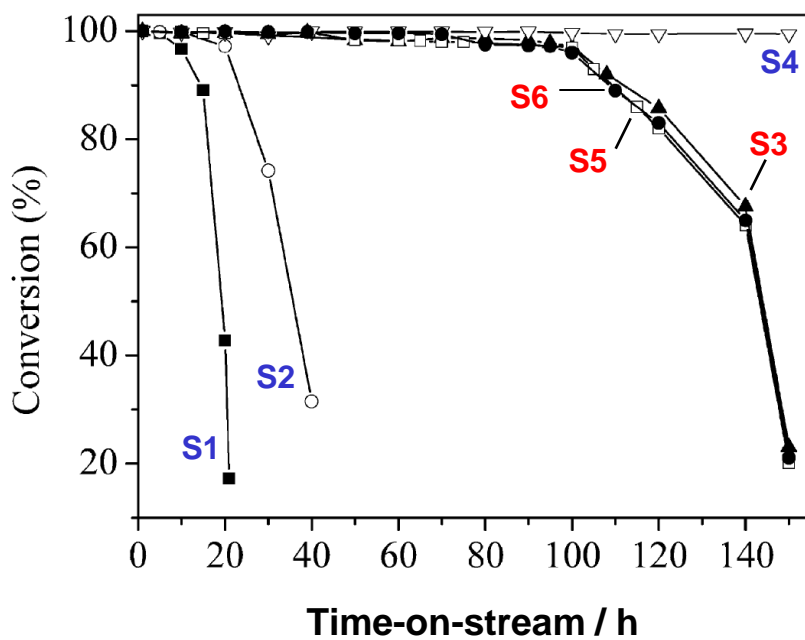




## V: Recent approaches for improved MTP catalysts

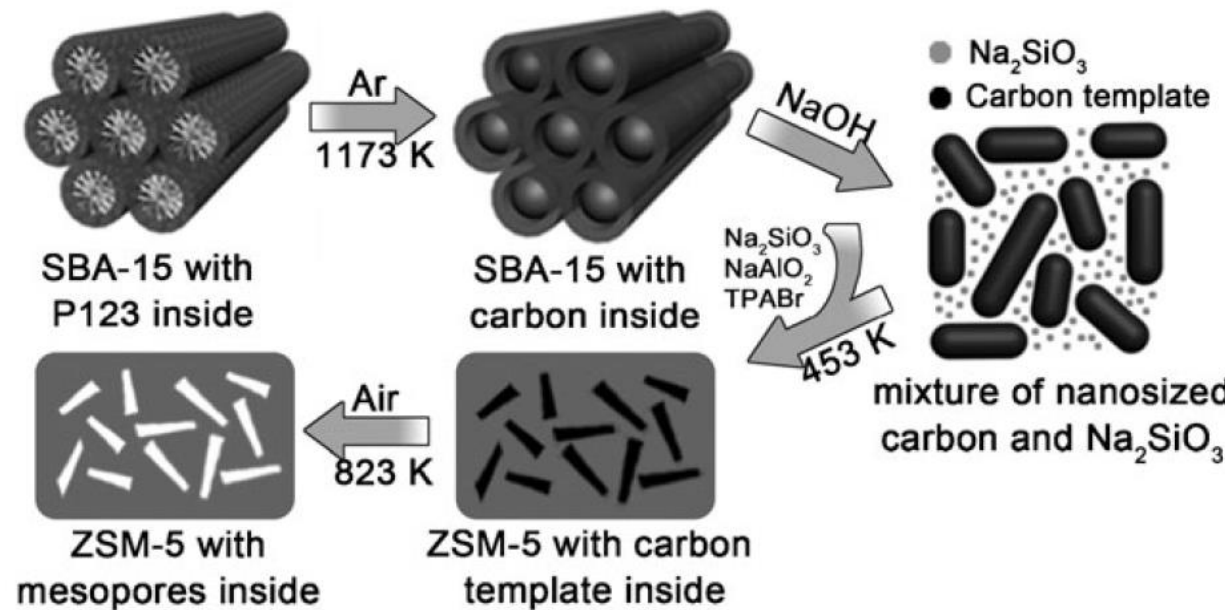
modification of high-silica ZSM-5 (**S3**:  $n_{\text{Si}}/n_{\text{Al}} = 72$ ) by treatment with 0.45 M  $\text{Na}_2\text{CO}_3$  and 1 M HCl (**S5**:  $n_{\text{Si}}/n_{\text{Al}} = 78$ ) and addition of starch to the synthesis gel (**S6**:  $n_{\text{Si}}/n_{\text{Al}} = 76$ ) (C. Mei, P. Wen, Z. Liu, Y. Wang, W. Yang, Z. Xie, W. Hua, Z. Gao, J. Catal. 258 (2008) 243)

methanol conversion at 743 K with  $\text{WHSV} = 1 \text{ h}^{-1}$  of different ZSM-5 samples (left) and product selectivities for sample **S5** (right)



## IV: Recent approaches for improved MTP catalysts

preparation of high-silica ZSM-5 with mesopores by addition of SBA-15 templated carbon nanoparticles to the zeolite synthesis gel (C. Sun et al., Chem. Commun. 46 (2010) 2671)



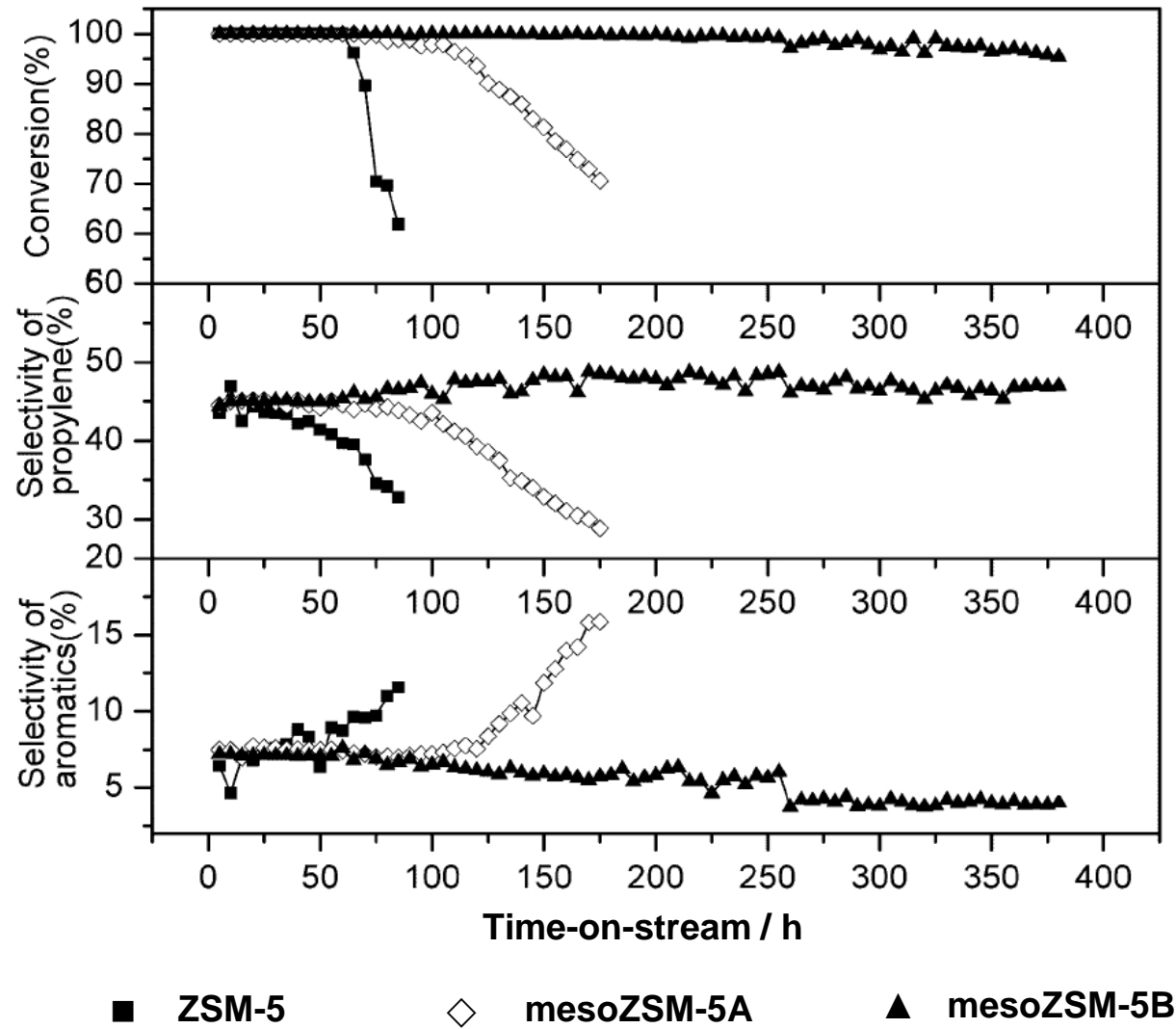
### textural properties of mesoporous ZSM-5:

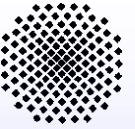
Sample	C/Si ratio <sup>a</sup>	$S_{\text{BET}}/\text{m}^2 \text{ g}^{-1}$	$V_{\text{micropore}}/\text{cm}^3 \text{ g}^{-1}$	$V_{\text{p total}}/\text{cm}^3 \text{ g}^{-1}$	Si/Al ratio <sup>b</sup>
ZSM-5	0	340	0.11	0.20	155
mesoZSM-5A	0.67	335	0.10	0.26	156
mesoZSM-5B	1.0	430	0.10	0.32	156



## V: Recent approaches for improved MTP catalysts

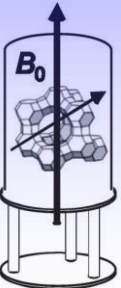
methanol conversion over mesoporous ZSM-5 at 733 K with WHSV = 1.25 h<sup>-1</sup>

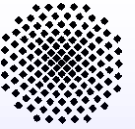




## ***Summary***

- depending on the level of impurities present in the methanol feed, methoxy groups may play a key role during the induction period
- the composition of the hydrocarbon pool formed under steady-state conditions depends on the type of zeolites (H-ZSM-5: more olefinic species; SAPO-34: more polymethylaromatics) and the reaction parameters
- adsorption of ammonia on used MTH catalysts gives information on number of accessible Brønsted acid sites and polyalkylbenzenium ions
- improvement of the lifetime of MTH catalysts requires further studies of microporous solids with one-dimensional pore system and medium acid site density and acid strength (e.g. silicoaluminophosphates)
- recent work on improved MTP catalysts focuses on high-silica ZSM-5 zeolites modified with phosphorus compounds and various approaches for obtaining mesopores





## *Thanks to ...*

### **co-workers:**

Thomas Horvath  
Michael Seiler  
Andreas Buchholz  
Udo Schenk  
Mingcan Xu  
Jiang Jiao  
Jun Huang  
Yijiao Jiang  
Jörg Frey  
Arne Bressel  
Reddy Marthala  
Bejoy Thomas  
Wei Wang  
Yean Sang Ooi  
Christian Lieder  
Harald Henning  
Weili Dai  
Zichun Wang  
u.a.

### **financial support:**

**Deutsche Forschungsgemeinschaft**  
**Fonds der Chemischen Industrie**  
**Volkswagen Foundation**  
**DECHEMA e.V.**  
**Alexander von Humboldt-Foundation**  
**u.a.**

